J|A|C|S
ARTICLES
Published on Web 01/10/2003

Dual Wavelength Parametric Test of Two-State Models for Circular Dichroism Spectra of Helical Polypeptides: Anomalous Dichroic Properties of Alanine-Rich Peptides

Peter Wallimann, Robert J. Kennedy, Justin S. Miller, William Shalongo, and Daniel S. Kemp*

Contribution from the Department of Chemistry, Room 18−296, Massachusetts Institute of Technology, Cambridge, Massachusetts 02139

Received July 2, 2002 ; E-mail: kemp@mit.edu.

Abstract: A two-state helix-coil model underlies all calculations of fractional helicities FH from CD spectra of helical polypeptides. The presence of an isodichroic point near 203 nm is widely assumed to validate this model, but is shown here to provide inadequate validation for alanine-rich peptides. A parametric correlation with constant slope *B* between CD ellipticities at a pair of wavelengths is introduced as a more rigorous two-state test. Correlations of temperature-dependent $[\theta]_{222}$ vs $[\theta]_{208}$ values are reported for a variety of peptides. Constant slopes *B* are observed for literature CD data obtained from fragments of helical proteins and dimeric helical coiled coils, but parametric correlations of CD data for alanine-rich peptides consistently exhibit anomalous concave upward curvature, characterized by local slopes that are linearly temperature dependent. Low-temperature CD studies together with parametric correlations at a series of wavelengths demonstrate that the curvature anomaly is maximal at 222 nm and localized in the 215−230 nm wavelength region. Precedented structural variation of the ϕ, ψ dihedral angles of the α-helix is suggested as a possible explanation. For the important case of alanine-rich peptides, experiments are proposed that may yield temperature corrections for $[\theta]_{222}$ and permit reliable calculations of FH from $[\theta]_{222}$ values.

Introduction

The backbone conformation of a peptide or protein defines its circular dichroism spectrum in the range 190−240 nm, providing a uniquely convenient tool for assigning secondary structure.[1] A dominant helical conformation is assigned if a distinctive helical CD signature is present. Fractional helicity, FH, the mole fraction of helical backbone α-carbons within the peptide or protein, is then often calculated as proportional to the experimental molar residue ellipticity at 222 nm, $[\theta]_{222}$.[2] These FH values derived from alanine-rich host peptides have been used to assign quantitative helical propensities for the natural amino acids, an important step toward predicting helicity from peptide amino acid sequences.[3] For the class of alanine-rich peptides, we have recently questioned the reliability of CD-derived FH assignments. Three years ago, we reported CD spectra for N-capped A_4K oligomers that exhibit anomalously large $[\theta]_{222}$ values, inconsistent with the conventional calculations that relate $[\theta]_{222}$ to FH.[4] This report addresses the scope, significant features, likely causes, and potential remedies for these anomalies.

A distinctive helical CD spectrum is characterized by a minimum at 208 nm, a second minimum of nearly equal intensity at 222 nm, and strong positive ellipticity at short wavelength that decreases and changes sign at ca. 200 nm.[1] A CD of a peptide with an unordered backbone conformation is characterized by strong negative ellipticity at short wavelength that decreases to zero near 210 nm. At longer wavelengths a weak maximum or minimum is frequently observed.[5]

Reversible melting in water of the native states of globular proteins to unfolded states can often be modeled accurately as a molecular two-state process,[6] conveniently monitored by CD.[7] The spectra usually resemble those of the idealized manifold of Figure 1; each of its spectra is calculated as a different ratio of CDs for completely helical and completely unstructured peptide conformations. The experimental temperature-dependent CD manifolds for simple helical peptides also resemble Figure 1, but at a molecular level peptide melting is not a two-state

(1) (a) Yang, J. T.; Wu, C.-S. C.; Martinez, H. M. *Methods Enzymol.* **1986**, *130*, 208−269. (b) Greenfield, N.; Fasman, G. D. *Biochemistry* **1969**, *8*, 4108−4116. (c) Woody, R. W. *Methods Enzymol.* **1995**, *246*, 34−71.
(2) (a) Marqusee, S.; Baldwin, R. L. *Proc. Natl. Acad. Sci. U.S.A.* **1987**, *84*, 8898−8902. (b) Jasanoff, A.; Fersht, A. R. *Biochemistry* **1994**, *33*, 2129−2135.
(3) (a) Rohl, C. A.; Baldwin, R. L. *Methods Enzymol.* **1998**, *295*, 1−26. (b) Park, S.-H.; Shalongo, W.; Stellwagen, R. *Biochemistry* **1993**, *32*, 7048−7053.
(4) Wallimann, P.; Kennedy, R. J.; Kemp, D. S. *Angew Chem., Int. Ed. Engl.* **1999**, *38*, 1290−1292.
(5) (a) Tiffany, M. L.; Krimm, S. *Biopolymers* **1972**, *11*, 2309−2316. (b) Woody, R. W. *Adv. Biophys. Chem.* **1992**: *96*, 37−79. (c) Park, S.-H.; Shalongo, W.; Stellwagen E. *Protein Sci.* **1997**, *6*, 1694− 1700.
(6) Dill, K. A.; Shortle, D. *Annu. Rev. Biochem.* **1991**, *60*, 795−825.
(7) The conformational population of the unstructured state changes with temperature and denaturant. The relative sensitivity of the measuring technique to structural changes in the native and unstructured states in part defines the adequacy of a two-state approximation. For melting of helical proteins CD measurements at 222 nm are particularly appropriate owing to the greater intensity of the helical dichroic chromophore, which minimizes the effects of temperature-dependent changes in the unstructured state.

10.1021/ja0275360 CCC: $25.00

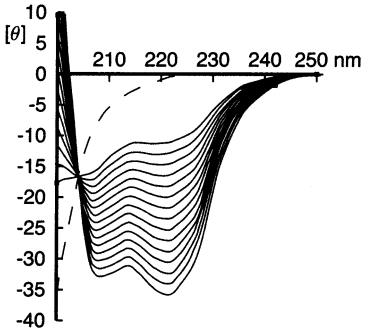

Figure 1. Idealized two-state helical CD manifold consisting of mixtures of completely helical (H) and unordered (U) peptide conformations. From top to bottom for $\lambda > 203$ nm, the curves correspond to increasing helical mole fraction: $\chi_H = 0$ (dotted line), and $0.3 \leq \chi_H \leq 1.0$ (solid lines) at increments of 0.05. Each curve is calculated as $[\theta] = [\theta]_U + ([\theta]_H - [\theta]_U)\chi_H$. Values for $[\theta]_U$ were calculated from 25 °C data of Figure 5; values for $[\theta]_H$ correspond to the CD of helical polyLys reported by Greenfield and Fasman.[1b] Ordinate ellipticity units: 10^3 deg cm^2 dmol^{-1}.

process. Why do helical proteins and peptides exhibit similar CD-monitored melting behavior?

Unlike the native state of a helical globular protein, the structured state of a simple helical peptide in water is an ensemble of rapidly equilibrating fully and partially helical conformations whose relative abundances show a complex dependence on temperature.[8] Helical proteins and peptides show qualitatively similar CD manifolds because both follow a two-state melting model based on the conformations at amino acid α-carbons. A conformation of either the helical peptide or the protein is defined by specifying for each of its α-carbons a sequence of pairs of ϕ, ψ dihedral angles. Each pair defines the relative orientation, helical or nonhelical, of the two amide residues that flank a particular α-carbon, and the interaction between these residues generates a local CD chromophore. Contiguous sequences of such helical chromophores interact further to generate the characteristic, intense helical CD signature,[1c] and the abundance-weighted ellipticity average over all residue chromophores approximates the experimental residue ellipticity $[\theta]$. The melting of a conformationally homogeneous native state of a helical protein can be modeled as a change in its mole fraction or equivalently in terms of the change in FH of its helical α-carbons. For the conformationally inhomogeneous helical state of a peptide, no currently available experimental method distinguishes partially helical conformations, and helicity modeling must monitor FH.

A progressive decrease in temperature is commonly used to increase FH for either proteins or peptides. Concomitant CD measurement then yields a CD manifold. Changes in protein conformation resulting from addition of salts or alcohol cosolvents, or from changes in pH, can be difficult to analyze, but for helically disposed simple peptides their effects on FH are less ambiguous, and these variables are often used in addition to temperature to generate CD manifolds.

Illustrated in Figure 1, an isodichroic point near 203 nm in a CD manifold of a peptide or protein has been the benchmark test[10] for a local two-state dichroic model that is applied to ellipticities at neighboring wavelengths. As noted by Holtzer and Holtzer, for either α-helical dimeric coiled coil proteins or a variety of helical peptides, a consistent ellipticity $-[\theta]_{203}$ of ca. 13 to 17 × 10^3 deg cm^2 dmol^{-1} is observed, and these authors propose its use as a convenient monitor of peptide concentration.[11] A 203 nm isodichroic point is often taken to validate a global two-state helix-coil ellipticity model that extends to 222 nm,[12] justifying calculation of FH from experimental $[\theta]_{222}$ values. For alanine-rich peptides, in the absence of independent supporting evidence, we question this assumption. A CD spectrum sums local ellipticity contributions, and the existence of an isodichroic point at short wavelength does not rule out contributions of local dichroic chromophores that significantly perturb ellipticity only at longer wavelengths. A more rigorous test of the two-state model is needed.

Parametric Two-Wavelength Test for a Two-State Dichroic Model

$$[\theta]_{exp} = [\theta]_U \cdot (1 - FH) + [\theta]_H \cdot FH = [\theta]_U + ([\theta]_H - [\theta]_U) \cdot FH \quad (1)$$

$$[\theta]_{exp,\lambda 1} = A + B \cdot [\theta]_{exp,\lambda 2} \quad (2)$$

$$B = \frac{[\theta]_{H,\lambda 1} - [\theta]_{U,\lambda 1}}{[\theta]_{H,\lambda 2} - [\theta]_{U,\lambda 2}} \qquad A = [\theta]_{U,\lambda 1} - B[\theta]_{U,\lambda 2} \quad (3)$$

For a helical peptide or protein that fits a two-state CD model, the familiar eq 1 relates the experimental residue ellipticity $[\theta]_{exp}$ at any wavelength to FH and limiting residue ellipticities $[\theta]_U$ and $[\theta]_H$, which respectively correspond to typical peptide residues in an unstructured region and in a helical region of length n. A CD manifold can be generated if FH and thus $[\theta]_{exp}$ depend on a progress variable such as temperature, and spectra are measured at a progressive series of its values. Equations 2 and 3 then result if eq 1 is rearranged to give FH as a function of $[\theta]_{exp}$ at a pair of wavelengths, and the resulting FH expressions are equated. Equations 2 and 3 imply that for a series of such pairs of $[\theta]_{exp}$, a parametric correlation must be linear, and the experimental slope B must be independent of the progress variable. This manuscript presents evidence that for alanine-rich peptides the parametric slopes B consistently show a strong dependence on temperature, implying that at least one assumption underlying eqs 1, 2, and 3 is invalid.

Any of three false assumptions could explain this failure. First, additional conformational states with nonhelical spectra and temperature dependences distinct from that of FH might contribute. Second, the expected weak correlation of $[\theta]_H$ with FH might generate a spurious temperature dependence for B.[13] (This effect should be nearly wavelength independent and relatively insignificant if a CD manifold exhibits a 203 nm isodichroic point.) Third, one or more of the four parameters

(8) Qian, H.; Schellman, J. A. *J. Phys. Chem.* **1992**, *96*, 3987−3994.
(9) The spacers $Inp_2{}^tL$ and ${}^tLInp_2$ confine the helix to the alanine region and define the maximum helical length of A_n, as in: Miller, J. S.; Kennedy, R. J.; Kemp, D. S. *J. Am. Chem. Soc.* **2002**, *124*, 945−962.
(10) See the Appendix for a discussion of this point.
(11) Holtzer, M. E.; Holtzer, A. *Biopolymers* **1992**, *32*, 1675−1677.
(12) (a) Nelson, J. W.; Kallenbach, N. R. *Proteins: Struct., Funct., Genet.* **1986**, *1*, 211−217. (b) Gans, P. J.; Lyu, P. C.; Manning, M. C.; Woody, R. W.; Kallenbach, N. R. *Biopolymers* **1991**, *31*, 1605−1614.
(13) For a helix of length n, the value of $[\theta]_H$ is usually taken as $[\theta]_{H\infty}(1 - X/n)$, where $[\theta]_{H\infty}$ corresponds to the residue ellipticity of a helical peptide of infinite length.[1] Though this value is appropriate for modeling helical proteins, we have shown previously that application of the Lifson−Roig model[8] to helical peptides rigorously requires that the value of $[\theta]_H$ correlate with FH, decreasing modestly with temperature.[9] As described in the Experimental Section, for the A_{28} peptide this effect on B is opposite in sign and roughly 3-fold smaller than that of a temperature-dependent $[\theta]_{U,222}$.

$[\theta]_H$ and $[\theta]_U$ might depend significantly upon temperature. These are the ellipticities observed or extrapolated for respective FH values of 1.0 or 0. Temperature-dependent changes in the conformations of the completely unstructured or completely helical states that occur independently of FH changes are the likely explanations for significant temperature dependence of either $[\theta]_H$ or $[\theta]_U$.

An unstructured state of a peptide is made up of distinct rapidly equilibrating conformations, and theory predicts small energy differences between them.[14] The resulting abundance-weighted average $[\theta]_U$ thus should show significant temperature dependence. Short peptides frequently assume unstructured states, and they are likely to be dominant under some denaturing conditions. Experimental models for $[\theta]_U$ are thus abundant, and these confirm the predictions of theory.[5b]

The arguments for or against structure-derived temperature dependences of $[\theta]_H$ are more complex. The structures of core-packed helical regions of globular proteins in their native states are well-defined by X-ray crystallography, and examples demonstrate the experimental invariance of their $[\theta]_{native}$ values to temperature changes within the region where χ_{native} approaches 1.0.[15] For these cases, the temperature dependence of $[\theta]_H$ usually is small or even undetectable. The complex structures of the conformational ensembles formed by helical peptides in solution have not been rigorously defined, and their $[\theta]_H$ values are currently controversial. A range of length dependent values have been proposed, and as discussed in a subsequent section, in some cases these have been assigned temperature dependences. For the purposes of this report, we regard the issue of the temperature dependence of $[\theta]_H$ for free helical peptides as unresolved, and that of $[\theta]_U$ as proven and defined by experiment

$$[\theta]_{exp} = [\theta]_U + ([\theta]_H - [\theta]_U)\cdot\epsilon \qquad 0 \sim FH = \epsilon \qquad (4)$$

$$[\theta]_{exp} = [\theta]_H - ([\theta]_H - [\theta]_U)\cdot\delta \qquad 1 \sim FH = (1 - \delta) \qquad (5)$$

What effects on $[\theta]_{exp}$ and B can be expected if either $[\theta]_H$ and $[\theta]_U$ is temperature dependent? From eq 1, these will clearly perturb $[\theta]_{exp}$, but the temperature dependence of FH itself is expected to dominate. Because B is the local slope of a parametric plot of two such $[\theta]_{exp}$ values, the effects on slope of the temperature dependence of FH largely cancel, and perturbations by temperature dependent $[\theta]_H$ and $[\theta]_U$ become dominant. The effects of these are best examined by a model that assumes eq 1 is valid at the wavelength $\lambda 2$, and both $[\theta]_{H,\lambda 2}$ and $[\theta]_{U,\lambda 2}$ are temperature independent. Two cases then arise: either the temperature dependence of $[\theta]_{U,\lambda 1}$ or that of $[\theta]_{H,\lambda 1}$ is dominant. Equations 4 and 5 apply if FH approaches limiting values. Inspection shows that if a temperature dependence of $[\theta]_{U,\lambda 1}$ is dominant, the perturbations in $[\theta]_{exp}$ will be nearly proportional to those in $[\theta]_{U,\lambda 1}$ if FH approaches 0, but they become insignificant as FH approaches 1. If temperature dependence of $[\theta]_{U,\lambda 1}$ dominates, an anomalous nonzero value of curvature will be largest at high temperatures and negligible at low temperatures.

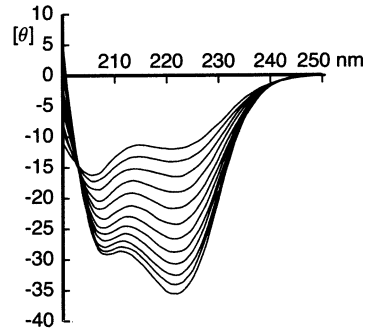

Figure 2. Experimental temperature-dependent CD manifold for spaced, solubilized Ala_{28} in water, $WK_4Inp_2{}^tLA_{28}{}^tLInp_2K_4NH_2$.[9] Inp = isonipecotic acid; ^tL = *tert*-leucine. From top to bottom for $\lambda > 203$ nm, the curves correspond to spectra at decreasing temperature, $60 \geq T \geq 5$ °C at 5 °C increments. Ordinate ellipticity units: 10^3 deg cm^2 dmol^{-1}.

As we are primarily interested in values of λ_1 greater than 210 nm, for which $[\theta]_{H,\lambda 1}$ is significantly more intense than $[\theta]_{U,\lambda 1}$, eq 5 implies that a dominant temperature dependence of $[\theta]_{H,\lambda 1}$ will perturb $[\theta]_{exp}$ and B equivalently at high values of FH (low temperatures) but the perturbation will remain large over most of the FH range. The experimental variation of slope with temperature seen in Figure 4 is consistent with this model, suggesting that temperature dependence of $[\theta]_H$ may be dominant.

Analysis of the Experimental Parametric $[\theta]_{222}$ vs $[\theta]_{208}$ Plot for A_{28} in Water. Temperature-dependent deviations from constant slope B can often be detected through simple visual inspection of the CD manifold. For example, in the manifold of Figure 1 at any pair of wavelengths the changes in $[\theta]$ seen in neighboring CD spectra are linearly correlated, and the forms of the spectra are related by a similarity transformation.

Figure 2 shows the experimental temperature dependent CD manifold for our previously reported[9] spaced solubilized polyalanine A_{28}. The spectra of this manifold show neither similarity nor proportionality. Although the calculated CD spectrum in Figure 1 for $\chi_H = 0.3$ closely resembles the experimental 60 °C spectrum of Figure 2, as the temperature is lowered, $[\theta]_{222}$ and $[\theta]_{208}$ change disproportionately, and corresponding spectra at lower temperatures and larger χ_H are increasingly dissimilar. A striking increase in the ratio $[\theta]_{222}/[\theta]_{208}$ appears for low-temperature spectra of Ala_{28} but is less evident at higher temperatures. This ratio R_2 was introduced in 1991 by Gierasch et al. as a measure of helicity.[16]

Figure 3 shows a parametric plot of $[\theta]_{222}$ vs $[\theta]_{208}$ for the data of Figure 2 and allows quantitation of the deviations from eq 3. Significant upward curvature is apparent throughout the temperature range, confirming that relative to $[\theta]_{208}$, the intensity of $[\theta]_{222}$ increases disproportionately as the temperature is lowered. Mean curvature is defined by Figure 4 which plots local tangents of Figure 3 vs the mean temperature of each tangent region. Within measurement error, the slope decreases nearly linearly with temperature, with an overall decrease of nearly 50%. If $[\theta]_{208}$ is proportional to FH throughout the temperature range, then $[\theta]_{222}$ is not. Extrapolating the slope of Figure 3 at high temperature demonstrates a low-temperature inconsistency in the value of $[\theta]_{222}$ of 12−15%, implying a corresponding uncertainty in a CD derived FH.

(14) Hodes, Z. I.; Nemethy, G.; Scheraga, H. A. *Biopolymers* **1979**, *18*, 1565−1610; Pettitt, B. M.; Karplus, M. *Chem. Phys. Lett.* **1985**, *121*, 194−201.
(15) Peterson, R. W.; Nicholson, E. M.; Thapar, R.; Klevit, R. E.; Scholtz, J. M. *J. Mol. Biol*. **1999**, *286*, 1609−1619. Holtzer, M. E.; Holtzer, A. *Biopolymers* **1992**, *32*, 1589−1591.
(16) Bruch, M. D.; Dhingra, M. M.; Gierasch, L. M. *Proteins: Struct., Funct., Genet.* **1991**, *10*, 130−139.

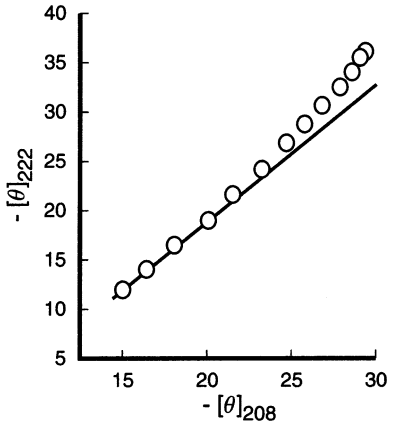

Figure 3. Parametric plot of $[\theta]_{222}$ vs $[\theta]_{208}$ for the Ala_{28} spaced solubilized peptide of Figure 2 over the temperature range of 60 (low $-[\theta]$ values) to 2 °C (high $-[\theta]$ values). Data points were measured at 2, 5 °C, and at 5 °C intervals to 60 °C. A linear regression line is shown for data at 45, 50, 55, and 60 °C. Ordinate ellipticity units: 10^3 deg cm^2 dmol^{-1}.

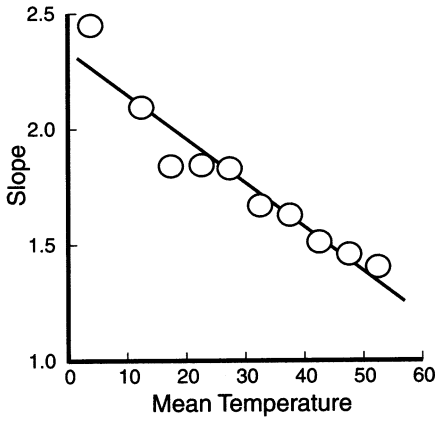

Figure 4. Plot of local slopes of Figure 3 vs mean local *T*. Slopes for linear regressions obtained from the temperature dependence of series of four consecutive $[\theta]$ data points of Figure 3 are shown as circles, with mean temperature varied from 3.5 to 52.5 °C. A linear regression of local slopes vs mean *T* has a correlation coefficient of −0.982.

A possible explanation is a significant temperature dependence of $[\theta]_U$ at either wavelength. Could this documented temperature dependence explain the slope changes of Figures 3 and 4? An answer begins with analysis of typical CD spectra for the unstructured state. Literature values for $[\theta]_U$ have been largely derived from studies of denatured polyLys,[1b] polyGlu,[17] N-hydroxyethylated polyGln,[18] and polyLeuLys,[19] although CD spectra of unstructured capped Ala_2 and Ala_3 peptides have also been reported.[20] The temperature-dependent CD manifold of Figure 5 contains twelve spectra of the spaced solubilized peptide $WK_4Inp_2{}^tLA_4{}^tLInp_2K_4NH_2$ in water at temperature increments of 5 °C.[9] It is representative of literature examples, and we use it in this study to model $[\theta]_U$, although it probably overestimates the value for Ala residues. Near 195 nm $[\theta]_U$ is strongly negative but decreases nearly linearly with increasing λ. Weak negative $[\theta]_U$ is observed in the region $208 \leq \lambda \leq 240$ nm; at lower temperatures $[\theta]_U$ exhibits a positive maximum at ca. 218 nm; $[\theta]_{U,222}$ is zero at ca. 25 °C, is negative between

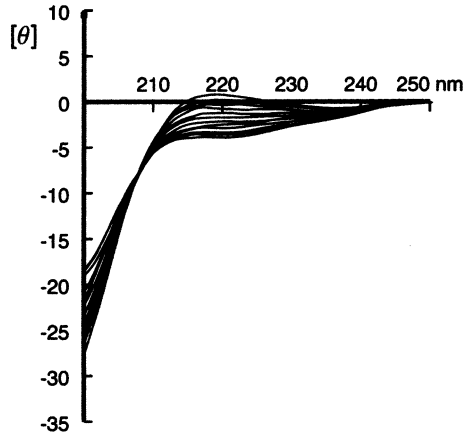

Figure 5. Temperature-dependent manifold of CD spectra in water at 5 °C intervals between 5 and 60 °C for $WK_4Inp_2{}^tLA_4{}^tLK_4NH_2$.[9] From top to bottom for $\lambda = 222$ nm, the curves correspond to spectra at increasing temperature. Lysine and alanine regions of these peptides are expected to assume unordered conformations. (See the Experimental Section) Ordinate ellipticity units: 10^3 deg cm^2 dmol^{-1}.

25 and 60 °C and increases linearly with temperature. Notably $[\theta]_{U,208}$ corresponds to a temperature-independent isodichroic point. For this reason and also owing to the high sensitivity of $[\theta]_{H,208}$ to changes in temperature or χ_{TFE}, we set the reference wavelength λ_2 equal to 208 nm for all tests of eq 3 in this report.

By setting $\lambda_1 = 222$ nm for A_{28} and using the Lifson−Roig equation[8] to model changes in slope *B* attributable to the temperature variation of $[\theta]_{U,222}$ seen in Figure 5, we can test whether this variation is sufficient to account for the slope change of Figure 4. As detailed in the Experimental Section, a temperature-dependent alanine helical propensity consistent with our earlier findings[9] was applied to a L−R model to calculate $[\theta]_{calcd,208}$ and $[\theta]_{calcd,222}$. Their linear regression yielded a 3-fold smaller change in modeled slope *B* than that observed in Figures 3 and 4, implying that the major part of their curvature cannot be attributed to a temperature dependence of $[\theta]_{U,222}$. By default, it must be attributed either to the CD contribution of an undefined new conformational state or, as we argue in a later section, to an anomalously large temperature dependence of $[\theta]_{H,222}$.

We address the following questions in the remainder of this report. How general are the slope changes of Figure 3? For what classes of peptides are they seen? What solvent changes influence them? If slope changes are observed, what is the range of their magnitudes and at what wavelength is the effect largest? What likely mechanism governs them? Are there any literature precedents? If slope changes are observed, can one modify calculation of FH from CD data to minimize error, and should one select $[\theta]_{222}$ or $[\theta]_{208}$ for optimal FH calculations?

Parametric $[\theta]_{222}$ vs $[\theta]_{208}$ Plots for Literature Helicity Data: Analysis of Temperature and TFE Dependences of CD Spectra of Dimeric α-Helical Coiled-Coils, Protein Fragments, and Alanine-Rich Designer Peptides. To address the generality of the anomalous temperature-dependent curvature of Figures 3 and 4, we turned first to literature CD manifolds that show a well-defined isodichroic point at 203 nm and that contain four or more spectra. Because only four to six spectra typically appear in each of these manifolds, their local curvatures could not be assigned accurately. Instead, a two-step criterion based on linear and quadratic fits to data was used to identify

(17) Rinaudo, M.; Domard, M. *J. Am. Chem. Soc.* **1976**, *98*, 6360−6364.
(18) Mattice, W. L.; Lo, J.-T.; Mandelkern, L. *Macromolecules* **1972**, *5*, 729−734.
(19) Brach, A.; Spach, G. *J. Am. Chem. Soc.* **1981**, *103*, 6319−6323.
(20) Mattice, W. L. *Biopolymers* **1974**, *13*, 169−183. Mattice, W. L.; Harrison, W. H. *Biopolymers* **1975**, *14*, 2025−2033.

cases suggestive of curvature. From a linear regression of $[\theta]_{exp,222}$ vs $[\theta]_{exp,208}$ we obtained a slope B and a standard deviation σ_{linear}, which was converted to a relative percentage error $100(\sigma_{linear}/\langle[\theta]_{222}\rangle)$. If this parameter fell below 2.5%, the data were deemed to be modeled successfully by eq 3. If this parameter exceeded 2.5%, we further tested for curvature by calculating $\sigma_{linear}/\sigma_{quad}$, where σ_{quad} is the standard deviation for a corresponding least-squares quadratic fit of $[\theta]_{222}$ vs $[\theta]_{208}$. For this ratio, we selected values greater than two as suggestive of curvature and grouped peptides with large ratios to identify structural features that correlate with curvature.

As noted above, $[\theta]_H$ values for proteins that assume native structures with dense hydrophobic interiors are unlikely to show large temperature dependences, and for these, linear $[\theta]_{222}$ vs $[\theta]_{208}$ plots are expected. Likely candidates are the dimeric α-helical coiled-coils, typified by the leucine zippers and tropomyosins. These are the simplest peptide-derived conformations that embody the essential features of a native conformation of a globular protein.[21] Coiled-coil amino acid sequences are characterized by a heptad repeat in which the hydrophobic amino acids Leu, Val, or Ile frequently appear at the first and fourth sites. Within the dimer these form a dense hydrophobic core of well-defined structure,[22] and they thus exhibit helix-coil transitions that are much more cooperative than those of isolated peptide helices. Although refined tests show that melting or denaturing transitions of dimeric coiled coils deviate from an ideal two-state model,[23] that model can approximate the requirements of a parametric CD correlation.[24]

Mo, Holtzer, and Holtzer[25] have reported temperature-dependent CD spectra for the dimeric helical coiled-coil formed by a nonpolymerizable rabbit cardiac tropomyosin. As seen in Figure 6, the data yield a linear parametric $[\theta]_{222}$ vs $[\theta]_{208}$ plot with fit parameters cited in the first entry of Table 1. As noted in the second entry of Table 1, an equally good linear correlation is seen for salt-dependent ellipticity changes reported for the same peptide

Peptide models for tropomyosins in the size range of 30−60 residues have been studied for more than a third of a century by Hodges, Kay, and their co-workers, and others have recently reported structural variants of similar length for the coiled-coil regions of the GCN4 leucine zipper protein. The third entry of Table 1 analyzes CD data taken from the study by Thompson et al.[24] of a 56 residue peptide fragment that includes the coiled-coil region of GCN4 plus a short portion of the basic DNA-binding region. The parametric ellipticity correlation of $[\theta]_{222}$ vs $[\theta]_{208}$ again is linear within error. From this data set, selected examples of correlations between $[\theta]_{208}$ and $[\theta]_\lambda$ values at shorter wavelengths were also analyzed and showed no curvature. The remaining less typical entries of Table 1 also exhibit

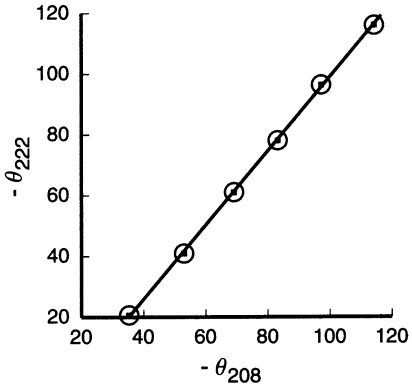

Figure 6. Parametric plot of θ_{222} vs. θ_{208}, with data of Mo, Holtzer, and Holtzer,[25] measured over the temperature range of 5 to 60 °C in benign aqueous media for rabbit cardiac tropomyosin (283 residues), modified to inhibit polymerization. Ellipticity units: millidegrees. Within measurement error, a linear correlation is observed. See Table 1 entry 1 for numerical analysis.

Table 1. Parametric $[\theta]_{222}$ vs $[\theta]_{208}$ Analysis for α-Helical Coiled-Coils

description	temp. or salt	range °C or M	no. of spectra	slope *B*	$(100\sigma_{Linear}/\langle[\theta]\rangle_{222}$
1. Mo[25]	t	5−60	6	1.22	−0.9
2. Mo[25]	s	0.03−0.13	4	1.17	−0.5
3. Thompson[24]	t	24−68	6	1.19	−0.9
4. Engel[26]	t	5−88	4	(1.90)	−1.9
5. Holtzer[27]	t	15−57	8	1.15	−2.0

parametric correlations that are linear within measurement error. The fourth entry analyzes data of Engel et al.[26] for a disulfide-linked dimer of a 39 residue coiled-coil peptide designed to form a hydrophobic core comprising 8 Ile residues. An anomalous isodichroic point was observed at ca. 210 nm, and the slope correlation was carried out between $[\theta]_{222}$ and $[\theta]_{212}$, where an ellipticity shoulder appeared. For these reasons, the slope B calculated for this case cannot be correlated with the other four examples. The final example of the Table analyzes temperature-dependent data reported by Holtzer et al.[27] for a novel retro-sequenced GCN4 analogue. Although the principal conformations detected for this substrate are monomer and tetramer, and other anomalous properties were observed, the error for a linear fit to the parametric plot lies within measurement limits, and the slope B falls within the range of the dimeric coiled coil examples of the Table

$$B = \frac{R_{2lim} - [\theta]_{U,222}/[\theta]_{H,208}}{1 - [\theta]_{U,208}/[\theta]_{H,208}} \qquad (6)$$

For highly helical peptides, R_{2lim}, the limit of the familiar ratio $R_2 = [\theta]_{222}/[\theta]_{208}$ as FH approaches 1.0, is slightly larger than 1.0.[28] R_{2lim} values of 1.06 to 1.09 can be calculated from canonical helical CD curves deconvoluted from protein CD and X-ray crystallographic data by linear least squares[1c,29] and SVD analyses,[30] by the convex constraint analysis,[31] and by more

(21) Kohn, W. D.; Hodges, R. S. *Trends Biotechnol.* **1998**, *16*, 379−389.
(22) (a) O'Shea, E. K.; Klemm, J. D.; Kim, P. S.; Alber, T. *Science* **1991**, *254*, 539−544. (b) Harbury, P. B.; Zhang, T.; Kim, P. S.; Alber, T. *Science* **1993**, *262*, 1401−1406. (c) Brown, J. H.; Kim, K.-H.; Jun. G.; Greenfield, N. J.; Dominguez, R.; Volkman, N.; Hitchcock-DiGregori, S. E.; Cohen, C. *Proc. Natl. Acad. Sci. U.S.A.* **2001**, *98*, 8496−8501.
(23) (a) Holtzer, A.; Holtzer, M. E.; Skolnick, J. In. *Protein Folding*; Gierasch, L. M., King, J., Eds.; AAAS Books: New York, 1990; pp 177−190. (b) Holtzer, M. E.; Lovitt, E. G.; d'Avignon, D. A.; Holtzer, A. *Biophys. J.* **1997**, *73*, 1031−1041. (c) Holtzer, M. E.; Braswell, E.; Angeletti, R. H.; Mints, L.; Zhu, D.; Holtzer, A. *Biophys. J.* **2000**, *78*, 2037−2048. (d) Muroga, Y.; Muraki, T.; Noda, I.; Tagawa, H.; Holtzer, A.; Holtzer, M. E. *J. Am. Chem. Soc.* **1995**, *117*, 5622−5626.
(24) Thompson, K. S.; Vinson, C. R.; Freire, E. *Biochemistry* **1993**, *32*, 5491−5496.
(25) Mo, J.; Holtzer, M. E.; Holtzer, A. *Biopolymers* **1990**, *30*, 921−927.
(26) Engel, M.; Williams, R. W.; Erickson, B. W. *Biochemistry* **1991**, *30*, 3161−3169.
(27) Holtzer, M. E.; Braswell, E.; Angeletti, R. H.; Mints, L.; Zhu, D.; Holtzer, A. *Biophys. J.* **2000**, *76*, 2037−2048.
(28) For a given peptide, R_{2lim} defines an upper limit for experimental R_2 values because, as is evident from Figure 5 and eq 1, as FH decreases, the corresponding decrease in intensity of $[\theta]_{exp,208}$ is less than that of $[\theta]_{exp,222}$. R_2 ratios calculated from Figure 1 demonstrates this effect.
(29) Greenfield, N. J. *Anal. Biochem.* **1996**, *236*, 1−10.

Table 2. Temperature-Dependent Parametric $[\theta]_{222} - [\theta]_{208}$ Analysis for Protein Fragments

description	range T °C	no. of spectra	slope B	$(100\sigma_{Linear}/\langle[\theta]\rangle_{222}$	$(\sigma_{Linear}/\sigma_{Quad})$
1. Lehrman A[38]	0−60	4	1.11	−0.7	
2. Lehrman B[38]	0−60	4	1.08	−0.3	
3. Lehrman C[38]	0−60	5	1.29	−1.6	
4. Lehrman D[38]	0−60	5	1.15	−2.2	1.4
5. Nelson[12a]	0−75	4	1.26	−5.0	1.2
6. Lim[39]	3−23	5	1.75	−2.4	1.1
7. Kuhlman[40]	1−85	4	1.37	−7.7	4.0

Table 3. χ_{TFE}-Dependent Parametric $[\theta]_{222}$ vs $[\theta]_{208}$ Analysis for Protein Fragments and Designer Peptides

description	χ_{TFE} range v/v%	no. of spectra	slope B	$100\sigma_{linear}/[\theta]_{222}$	$\sigma_{linear}/\sigma_{quad}$
1. Jasanoff[2b]	0−21	7	1.22	−2.3	
2. Dyson[41]	0−40	4	1.11	−2.3	
3. Gronenborn[42]	0−50	6	1.47	−1.8	
4. Shin[43]	0−80	5	1.16	−10[a]	0.89
5. Sonnichsen[44]	0−80	5	1.08	−2.4	1.8
6.Viguera[45]	0−25	4	1.29	−7.4	3.4[b]
7. Shin[43]	0−50	6	1.07	−4.3	9.0[b]
8. Forood[46]	0−14	5	1.24	-4.1	9.0[b]

[a] The large percent error in slope seen for this peptide results primarily from its exceptionally weak ellipticity. [b] Concave downward curvature was observed.

recent methods.[32] The R_{2lim} values of tropomyosins lie close to 1.00,[25] and peptide tropomyosin models and leucine zipper analogues generally show R_{2lim} values in water or another benign medium in the range of 1.0−1.05,[33] although values as high as 1.14 have occasionally been reported.[34] These ratios should be applied with caution to unassociated peptides. Cooper and Woody have calculated that formation of a dimeric helical coiled coil from a simple α-helix should diminish the intensity of the CD parallel $\pi-\pi^*$ transition and increase the intensity of the 222 nm n-π^* transition.[35] Empirical R_2 values derived from study of structurally well-defined helical coiled coils may not provide good models for helices formed by simple unaggregated peptides. Transformation of eq 3 yields eq 6, which links the slope B of the plot of $[\theta]_{222}$ vs.$[\theta]_{208}$ with R_{2lim} for a case in which little or no curvature is demonstrable. For R_{2lim} in the range of 1.0−1.05, assigning values[36] for $[\theta]_U$ from data of Figure 5 and setting $[\theta]_{H,222} = -37$ as proposed by Besley and Hirst from the protein database,[37] one can estimate B as 1.25 (SD 0.1). This value may also apply to a local slope B calculated from CD data for highly helical peptides. Values of B that grossly exceed this range are likely to reflect anomalously large values for R_{2lim}.

CD analysis of dilute aqueous solutions of unaggregated peptide fragments derived from helical regions of globular proteins provide most of the temperature-dependent manifolds of Table 2. These fragments lack core protein packing that enhances and defines their conformations within native proteins. For these sequences, $[\theta]_H$ may exhibit temperature dependence. The parametric comparisons of $[\theta]_{222}$ vs $[\theta]_{208}$ values seen in Table 2 test whether CDs of natural helical peptide fragments obey eqs 2 and 3 when studied out of their native contexts. The first four entries of Table 2 analyze CD spectra reported by Lehrman et al.[38] and measured for fragments selected from helical regions of bovine growth hormone. Significantly, all give normal values of the slope parameter B, and all give acceptable linear correlations of $[\theta]_{222}$ vs $[\theta]_{208}$. Entry five of Table 2 analyzes the temperature-dependent CD manifold of the helical ribonuclease S-peptide in 10 mol % TFE (trifluoroethanol) as reported by Nelson et al.,[12a] and entry six analyses a manifold of an analogue that is N-capped by a helix-stabilizing succinate function.[39] Both yield acceptable linear correlations.

The CD manifold of the final peptide example in Table 2 was reported by Kuhlman et al.[40] and tests a special issue. This peptide corresponds to a 34 residue α-helical region that spans two compact globular domains of the ribosomal protein L9. Its central region lacks significant core packing within the native state, and the complete peptide shows exceptional helical stability in isolation in water. The sequence is largely made up of Ala, Lys, Gln, Leu, and Glu residues, all strong helix formers. The authors tentatively attribute the high helicity to this amino acid composition and to the presence of charged residues that are properly sited for helix stabilization. They also note the likely significance of an absence of helix-destabilizing β-branched amino acids. Within the small group of literature-derived native peptides that we have thus far examined, this sequence is unique in exhibiting easily detectable parametric curvature. Table 3 presents results of analyses of CD manifolds that have been reported for TFE titrations of two alanine-rich designer peptides and six natural peptide sequences. The first three entries analyze data for short natural and designer peptides reported by Jasenoff and Fersht,[2b] Dyson et al.,[41] and Gronenborn, Bovermann, and Clore.[42] These yield acceptable linear correlations, as do the following pair of examples, which are derived from study of a 25-residue fragment of sperm whale myoglobin reported by Shin et al.[43] and from a correlated CD and NMR study by Sonnichsen et al.[44] of TFE-induced helicity of a 20-residue actin fragment. Curvature is demonstrable for the remaining three analyses of data reported for a second myoglobin fragment studied by Shin et al.,[42] an alanine-rich designer peptide of Viguera and Serrano,[45] and an N-cap stabilized alanine-rich peptide studied by Forood, Feliciano, and Nambiar.[46] Thus five out of six

(30) Compton, L. A.; Johnson, W. C., Jr. *Anal. Biochem.* **1986**, *155*, 155−167. Manavalan, P.; Johnson, W. C., Jr. *Anal. Biochem.* **1987**, *167*, 76−85; Johnson, W. C. *Proteins, Struct., Funct., Genet.* **1999**, *35*, 307−312.
(31) Perczel, A.; Hollosi, M.; Tusnady, G.; Fasman, G. D. *Protein Eng.* **1991**, *4*, 669−679.
(32) Sreerama, N.; Woody, R. A. *Anal. Biochem.* **2000**, *287*, 282−260.
(33) (a) Lau, S. Y. M.; Taneja, A. K.; Hodges, R. S. *J. Biol. Chem.* **1984**, *259*, 13 253−13 261. (b) Zhou, N. E.; Kay, C. M.; Hodges, R. S. *J. Biol. Chem.* **1992**, *267*, 2664−2670. (c) Lu, M.; Shu, W.; Ji, H.; Spek, E.; Wang, L.; Kallenbach, N. R. *J. Mol. Biol* **1999**, *288*, 743−752.
(34) Houston, M. E., Jr.; Wallace, A.; Bianchi, E.; Pessi, A., Hodges, R. S. *J. Mol. Biol*, **1996**, *262*, 270−282. (b)Lee, D. L.; Lavigne, P.; Hodges, R. S. *J. Mol. Biol.* **2001**, *306*, 539−553.
(35) Cooper, T. M.; Woody, R. W. *Biopolymers* **1990**, *30*, 657−676.
(36) In units of 10^3 deg cm^2 dmol^{-1}.
(37) Besley, N. A.; Hirst, J. D. *J. Am. Chem. Soc.* **1999**, *121*, 9636−9644.
(38) Lehrman, S. R.; Tuls, J. L.; Lund, M. *Biochemistry* **1990**, *29*, 5590−5596. Labels correspond to those in Figure 4 of their report.
(39) Lim, D.; Moye-Sherman, D.; Ham, I.; Jin, S.; Burgess, K.; Scholtz, J. M. *Chem. Commun.* **1998**, 2375−2376.
(40) Kuhlman, B.; Yang. H. Y.; Boice, J. A.; Fairman, R.; Raleigh, D. P. *J. Mol. Biol.* **1997**, *270*, 640−647.
(41) Dyson, H. J.; Rance, M.; Houghten, R. A.; Wright, P. E.; Lerner, R. A. *J. Mol. Biol.* **1988**, *201*, 201−217.
(42) Gronenborn, A. M.; Bovermann, G.; Clore, G. M. *FEBS Lett.* **1987**, *215*, 88−94.
(43) Shin, H.-C.; Merutka, G.; Waltho, J. P.; Wright, P. E.; Dyson, H. J. *Biochemistry* **1993**, *32*, 6348− 6355.Shin, H.-C.; Merutka, G.; Waltho, J. P.; Tennant, L. L.; Dyson, H. J.; Wright, P. E. *Biochemistry* **1993**, *32*, 6356−6364.
(44) Sonnichsen, F. D.; Van Eyk, J. E.; Hodges, R. S.; Sykes, B. D. *Biochemistry* **1992**, *31*, 8790−8798.
(45) Viguera, A. R.; Serrano, L. *Biochemistry* **1995**, *34*, 8771−8779.
(46) Forood, B.; Feliciano, E. J.; Nambiar, K. P. *Proc. Natl. Acad. Sci. U.S.A.* **1993**, *90*, 838−842.

Table 4. Temperature-Dependent Parametric $[\theta]_{222}$ vs $[\theta]_{208}$ Analysis for Designer Peptides

description	*T* range °C	no. of spectra	slope *B*	$100\sigma_{Linear}/[\theta]_{222}$	$\sigma_{Linear}/\sigma_{Quad}$
1. Kallenbach[12b,47]	1−90	4	1.44	−1.5	1.0
2. Kallenbach[12b,47]	4−90	4	1.58	−2.5	1.7
3. Jackson[48]	0−80	5	1.77	−5.0[a]	1.75
4. Ala_{28}[9]	5−60	6	1.64	−2.8	2.3
5. Merutka[49a]	0−96	7	1.56	−8.0[b]	3.5
6. $AcHel(A_4K)_4A_2NH_2$[4]	−20−60	17	2.12	−3.4[b]	4.0
7. Merutka[49b]	1−85	6	1.46	−3.8[b]	5.0
8. Baldwin[3a]	1−70	4	1.46	−6.0[b]	6.8

[a] Alanine rich but constrained by a covalent intrahelical loop. [b] Alanine-rich peptide.

naturally derived peptide fragments of Table 3 give an acceptable linear correlation, but both alanine-rich designer peptides fail a linearity test. The curvature seen in Figures 3 and 4 for the helical Ala_{28} peptide is clearly atypical for dimeric helical coiled coils or for protein fragments but not for alanine-rich peptides.

The literature contains many examples of helical peptides constructed by design. Representative temperature-dependent CD manifolds for these are analyzed in Table 4, which includes for comparison a corresponding analysis of the Ala_{28} peptide and our previously characterized cap-stabilized Baldwin-Marqusee peptide $AcHel(A_4K)_4A_2NH_2$.[4] The first two entries of Table 4 report results of curvature analysis of temperature-dependent CD spectra of the peptide sequence succinyl-$YSE_4K_4X_3E_4K_4NH_2$ developed and studied by the Kallenbach group to test helical propensities of a range of X residues.[47] For the first entry, the X_3 sequence is Ala_3; for the second, the sequence is LeuGlyLeu. Neither peptide is alanine-rich, and the CD manifolds for both yield acceptable parametric linear slope correlations.

The third entry of Table 4 reports analysis of CD data for a peptide for which nine of sixteen residues are alanine.[48] However, the helix formed by this peptide is stabilized by an *i*, *i* + 7 covalent bridge that might be argued to play the conformation-restricting role of the packing constraint of the hydrophobic core of a globular protein or of a helical coiled coil. Although the relative error of linear fit for this peptide is high, curvature is not convincingly demonstrated. All other CD manifolds analyzed in the Table were measured for alanine-rich designer peptides or polyalanines, and all show evidence for concave upward curvature, which in many cases is considerably larger than that exhibited by Ala_{28}. The CD data used for the eighth analysis was taken from the report of Marqusee and Baldwin[3a] for the sequence $AcA(EA_3K)_3ANH_2$, which was also studied by Merutka and Stellwagen,[49a] whose data are analyzed in the fifth example. Data for the seventh analyses were reported by the Stellwagen group for the sequence $AcW(EA_3R)_3A-NH_2$.[48b] The substantial curvature implied by the ratio of linear to quadratic errors for this case is demonstrated in Figure 7.

Analyses of nineteen examples of CD manifolds for helical coiled coils and helical peptides that are not alanine-rich appear in Tables 1 to 4. Only two show evidence of curvature, and the average slope *B* for the remainder is 1.23 (SD 0.16), within a

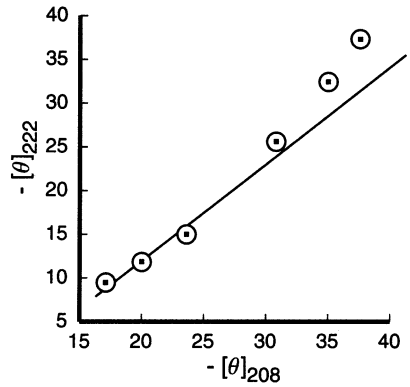

Figure 7. Parametric plot of $[\theta]_{222}$ vs $[\theta]_{208}$ data of Merutka, Shalongo, and Stellwagen,[49b] measured over the temperature range from 0 to 96 °C in water for the alanine-rich helical designer peptide $AcW(EA_3R)_3NH_2$. Substantial concave upward curvature is evident. Ordinate units: 10^3 deg cm^2 dmol^{-1}.

normal range. Large curvatures and high slopes for parametric plots imply corresponding errors and uncertainties for conventional calculations of fractional helicities from experimental values of $[\theta]_{222}$, but the above analyses suggest that these calculations are reliable if applied to most heterogeneous amino acid sequences. The case for the alanine-rich peptides of Tables 1−4 is very different. The analysis of one CD manifold falls just below the curvature cutoff, but the remainder show curvature, with a markedly abnormal average slope *B* of 1.63 (SD 0.23). The maximum slope was observed for cap-stabilized $AcHel(Ala_4Lys)_4Ala_2NH_2$, which exhibits intense low-temperature $[\theta]_{222}$ values that exceed calculated maximum standards.[4]

FH values derived from CD host−guest studies of polyalanines are natural choices for constructing and testing algorithms that predict helicity from amino acid composition and sequence, but for such modeling a rigorous recalibration is required to meet minimal standards of accuracy. The analysis of the next section provides a necessary first step toward that recalibration.

Analysis of CD Manifolds for Polyalanines and Ala_4Lys Oligomers; Dependence of Anomalous Curvature for Plots of $[\theta]_\lambda$ vs $[\theta]_{208}$ on Temperature, Length, Solvent, Capping, and λ. In this section, we analyze temperature-dependent helical CD data in aqueous media for a series of polyalanines and for an alanine-rich peptide, studied with and without a strongly helix-stabilizing N-cap. For the latter cases, the solvent was also varied to include ethylene glycol EG or the helix stabilizing alcohol trifluoroethanol TFE. These studies of alanine-rich peptides addressed a series of questions. For their temperature-dependent CD manifolds, are parametric $[\theta]_{222}$ vs $[\theta]_{208}$ plots invariably curved? If not, is curvature invariably found for peptides that under optimal conditions exhibit intense $[\theta]_{222}$ values, exceeding current limits? If curvature is observed, in what wavelength region does it appear and at what wavelength is it maximal?

In the introductory section of this report, we analyzed a helical CD manifold for the spaced, solubilized polyalanine A_{28} in water to obtain the data of Figures 3 and 4. By invalidating a quantitative two-state CD helicity model, these data established polyalanines of sufficient length as an archetype for curved

(47) (a) Lyu, P. C.; Liff, M. I.; Marky, L. A.; Kallenbach, N. R. *Science* **1990**, *250*, 669−673. (b) Lyu, P. C.; Wang, P. C.; Liff, M. I.; Kallenbach, N. R. *J. Am. Chem. Soc.* **1991**, *113*, 3568−3572.
(48) Jackson, D. Y.; King, D. S.; Chmielewski, J.; Singh, S.; Schultz, P. G. *J. Am. Chem. Soc.* **1991**, *113*, 9391−9392.
(49) (a) Merutka, G.; Stellwagen, E. *Biochemistry* **1990**, *29*, 894−898. (b) Merutka, G.; Shalongo, W.; Stellwagen, E. *Biochemistry* **1991**, *30*, 4245−4248.(c) Merutka, E.; Stellwagen, E. *Biochemistry* **1991**, *30*, 1591−1594.

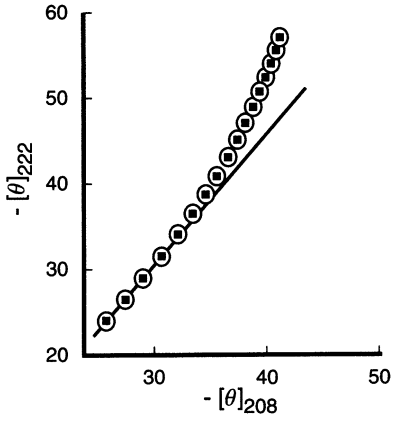

Figure 8. Parametric plot of $[\theta]_{222}$ vs $[\theta]_{208}$ for AcHel$(Ala_4Lys)_4Ala_2NH_2$ in 16 mol % EG-water over the temperature range of 60 (low $-[\theta]$ values) to -20 °C (high $-[\theta]$ values), ΔT of 5 °C. The line corresponds to a linear regression of the data measured at 45, 50, 55, and 60 °C. Ordinate ellipticity units: 10^3 deg cm^2 dmol^{-1}. EG = ethylene glycol.

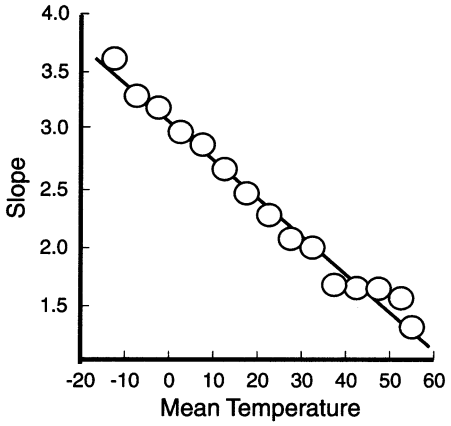

Figure 9. Plot of local slopes of Figure 8 vs *T*. Linear regressions obtained from the temperature dependence of series of four groups of consecutive data points of Figure 8 are shown as circles, with mean temperature varied from -12.5 to 52.5 °C. The average curvature of Figure 8 is shown as a linear regression line, which has a CC of -0.993.

parametric ellipticity correlations. The cap-stabilized Baldwin−Marqusee peptide AcHel$(Ala_4Lys)_4Ala_2NH_2$ was the first peptide for which anomalously intense helical CD spectra were reported.[4] We now show that this peptide also shows parametric curvature and define it as a second archetype.

The CD manifold of Figure 10B contains 17 spectra measured between -20 to 60 °C for AcHel$(Ala_4Lys)_4Ala_2NH_2$ in 16 mol % EG-water. Results of a parametric $[\theta]_{222}$ vs $[\theta]_{208}$ correlation are shown in Figures 8 and 9. A qualitative comparison shows that Figures 3 and 8 and Figures 4 and 9 are similar, but as expected for its larger range, the overall change in curvature of Figure 8 exceeds that of Figure 3. Later in this section, a quantitative curvature parameter is introduced that corrects for range.

These curvature archetypes are both alanine-rich, but their peptide sequences are different, they bear different caps, and different solvents were used for CD measurements. Are the similarities of Figures 3 and 8 coincidental? A brief analysis introduces this issue which is discussed in detail at the close of the section. The factors that stabilize the homoalanine helix are straightforward. The pair of solubilizing and isolating caps of A_{28} interact weakly with it and are slightly helix destabilizing.[50] The properties of helical conformations of this spaced, solubilized homopeptide thus must reflect the intrinsic properties of helices formed by alanine, which is structurally the simplest of the strongly helix-stabilizing amino acids. From Lifson-Roig analysis the conformational ensemble of A_{28} must be frayed, and its FH values are expected to fall significantly below 1.0. Nevertheless, near 0 °C, its value for $[\theta]_{222}$ lies close to the maximum calculated from conventional ellipticity functions.[51,12b,52] This polyalanine archetype displays parametric curvature, and at low temperatures exhibits anomalously large R_2 values and intense, nonstandard $[\theta]_{222}$ values.

The factors that stabilize the AcHel$(Ala_4Lys)_4Ala_2NH_2$ helix are more complex. Its Lys residues may interact strongly with the helix and alter CD spectra.[53] It has recently been suggested that EG may play a similar role.[54] As an exceptionally strong stabilizing N-cap, AcHel might change the fundamental character of an alanine-rich conformational ensemble unpredictably.[55]

A visual synopsis of our temperature-dependent CD manifolds for alanine-rich peptides appears in Figures 2, 10, 11, 12, and 13. Pairwise comparisons of Figures 10 & 11ABCD allow analysis of properties of N-capped and free forms of $(Ala_4Lys)_4Ala_2NH_2$ in water and EG-water. Figures 11D and 13 allow comparison of manifolds measured in water for $(Ala_4Lys)_4Ala_2NH_2$ with the spaced, solubilized polyalanine A_{19}; their low-temperature CD spectra show comparable $[\theta]_{222}$ values. All these manifolds exhibit nonlinear $[\theta]_{222}$ vs $[\theta]_{208}$ correlations and all cap-stabilized helices exhibit anomalously large R_2 values at low temperatures.

We previously demonstrated nearly superimposable CD spectra for nontemplated peptides measured at low temperatures that are paired with corresponding AcHel peptides measured at temperatures raised by 30−40 °C.[4] AcHel stabilizes helices without significant change in their CD properties. Similar comparisons follow from Figures 11A and B and Figures 11C and D. The presence of the AcHel cap substantially increases FH, but it cannot be the primary cause of curvature, which is also independent of the presence or absence of Lys residues or of the antifreeze additive EG.

Table 5 presents quantitative analyses of correlations of local slopes for $[\theta]_{222}$ vs $[\theta]_{208}$ for the CD manifolds of Figures 2, 3, 4, 8, 9, 10, 11, and 13. In the previous section, three criteria were used to identify parametric curvature in CD manifolds; a large slope B of a parametric plot, a relative linear error in fit $100\sigma_{linear}/\langle[\theta]_{222}\rangle$ for that plot, and a large SD ratio of errors of quadratic and linear fits. The first two of these are listed in columns three and four of Table 5. Comparisons of the slopes *B* of the third column of the Table with those of Tables 1 to 4 show that with the exception of the weakly helical peptide A_{16}, all show large *B* values, implying abnormally large values for R_{2lim}. For CD manifolds of Table 5 that are analyzed over the temperature range of 5 to 60 °C, the mean *B* value for AcHel

(50) Maison, W.; Kennedy, R. J.; Miller, J. S.; Kemp, D. S. *Tetrahedron Lett.* **2001**, *42*, 4975−4977.
(51) The maximum literature $[\theta]_H$ value for a completely helical peptide of length 28, −40 000, was calculated as in ref 12, setting $[\theta]_{H\infty}$ equal to −44 000 deg cm^{2}dm^{-1} [12b,52]
(52) Luo, P.; Baldwin, R. L. *Biochemistry* **1997**, *36*, 8413−8421.
(53) Grobke, K.; Renold, P.; Tsang, K.-Y.; Allen, T. J.; McClure, K.; Kemp, D. S. *Proc. Natl. Acad. Sci. U.S.A.* **1996**, *93*, 4025−4029.
(54) Dang, Z.; Hirst, J. D. *Angew. Chem., Int. Ed. Engl.* **2001**, *40*, 3619−3622.
(55) (a) Rohl, C. A.; Fiori, W.; Baldwin, R. L. *Proc. Natl. Acad. Sci. U.S.A.* **1999**, *96*, 3682−3687. (b) Spek, E. J.; Olson, C. A.; Shi, Z.; Kallenbach, N. R. *J. Am. Chem. Soc.* **1999**, *121*, 5571−5572; but see also (c): Kennedy, R. J.; Tsang, K.-Y.; Kemp, D. S. *J. Am. Chem. Soc.* **2002**, *124*, 934−944.

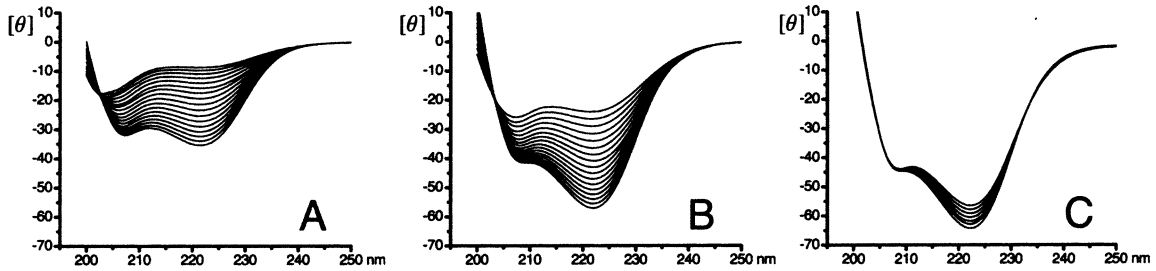

Figure 10. Temperature-dependent CD manifolds in EG−water mixtures for $(Ala_4Lys)_4Ala_2NH_2$ peptides. Spectra were measured at 5 °C intervals; at 222 nm from top to bottom, spectra appear in order of decreasing temperatures. Ellipticity units: 10^3 deg cm^2 dmol^{-1}A. $H_2^+(Ala_4Lys)_4Ala_2NH_2$ in 16 mol % EG−water 60 to −20 °C. B. AcHel$(Ala_4Lys)_4Ala_2NH_2$ in 16 mol % EG−water 60 to −20 °C. C. AcHel$(Ala_4Lys)_4Ala_2NH_2$ in 32 mol % EG−water −20 to −50 °C.

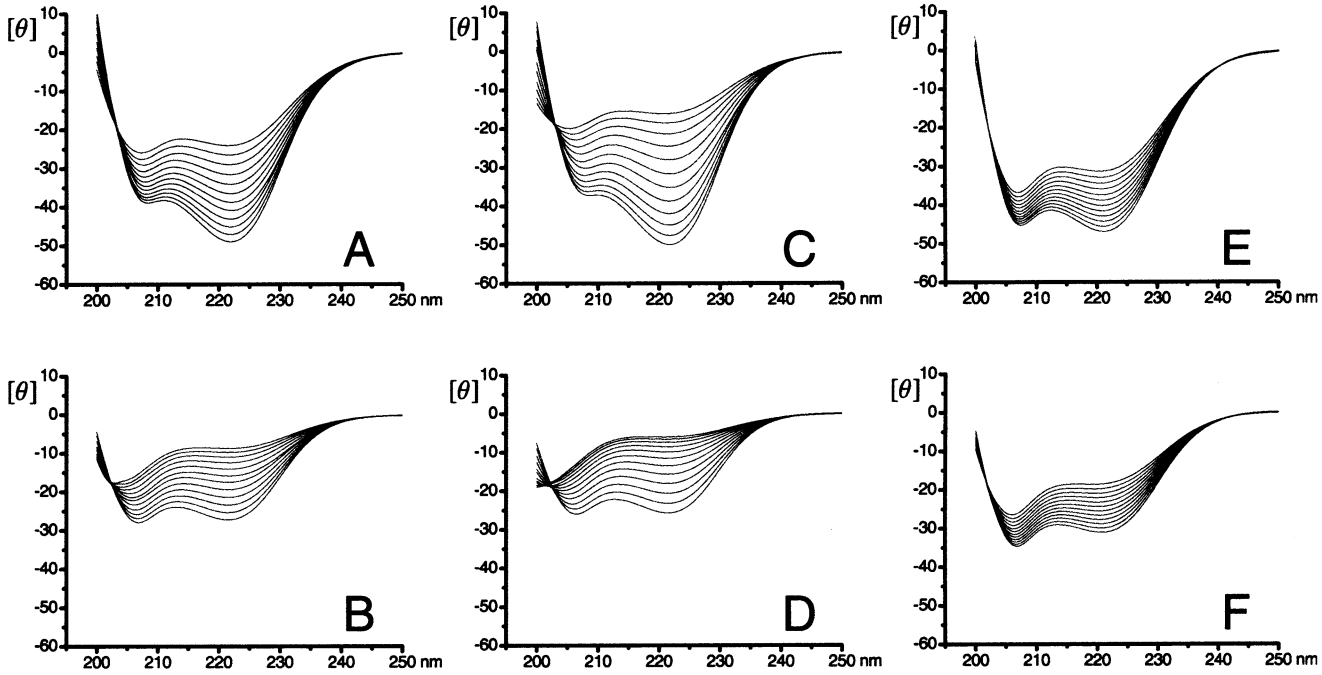

Figure 11. Temperature-dependent CD manifolds in aqueous mixtures from 5 to 60 °C for $(Ala_4Lys)_4Ala_2NH_2$ peptides. Spectra were measured at 5 °C intervals; at 222 nm from top to bottom, spectra appear in order of decreasing temperatures. Ellipticity units: 10^3 deg cm^2 dmol^{-1}. A, C, and E show AcHel$(Ala_4Lys)_4Ala_2NH_2$ CD spectra: B, D, F, show corresponding $H_2^+(Ala_4Lys)_4Ala_2NH_2$ spectra; Solvent compositions: A & B: 16 mol % EG-0.02 M aqueous perchlorate; C & D: 0.2 M aqueous perchlorate; E & F 16 mol % TFE−0.1 M aqueous perchlorate EG = ethylene glycol; TFE = trifluoroethanol.

capped peptides is 2.0, while that for the corresponding uncapped peptides is 1.7, which may be compared with the value of 1.6 found for the A_{28} and A_{19} peptides. High, temperature-dependent slopes of parametric $[\theta]_{222} - [\theta]_{208}$ plots thus appear to be a fundamental characteristic for all highly helical alanine-rich peptides of this study.

The large number of spectra in each CD manifold of Table 5 permits quantitative assignment of local curvature and its temperature-dependence $B(T)$. (As in other tables, the least squares slope calculated over the temperature range of the study is tabulated as average slope B.) As seen in Figures 4 & 9, the dependence of local slope on temperature is linear within measurement error. The correlation coefficients CC that quantitatively address this point appear in the last column of Table 5. For longer peptide sequences and for all peptides bearing the AcHel cap, values for CC lie in the range −0.98 to −1.0. The sixth column of the Table lists relative curvature, expressed averaged local curvature $\langle \Delta B(T)/\Delta T \rangle$ divided by B. For uncapped peptides its value is $\sim -9 \times 10^{-3}$ K^{-1}; for AcHel-capped peptides it is ca. 30% larger. Caution must be used in extrapolating these parameters outside the temperature ranges

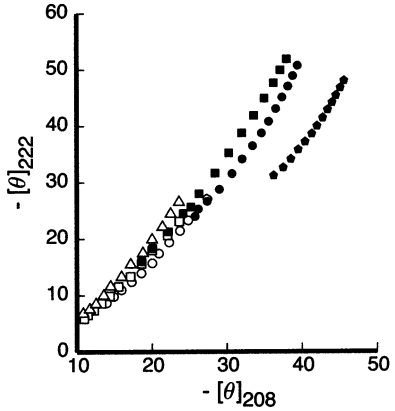

Figure 12. Parametric plots of $[\theta]_{222}$ vs $[\theta]_{208}$ data from Figures 11 & 13 Closed symbols correspond to AcHel capped peptides. Squares correspond to $(Ala_4Lys)_4Ala_2NH_2$ peptides in 16 mol % EG-0.02 M aqueous perchlorate; circles to $(Ala_4Lys)_4Ala_2NH_2$ peptides in 0.2 M aqueous perchlorate; triangles to the A_{19} peptide of Figure 13 in water; pentagons to the AcHel$(Ala_4Lys)_4Ala_2NH_2$ peptide in 16 mol % TFE−0.1 M aqueous perchlorate.

of this study. At sufficiently high or low temperatures, FH is expected to approach its limiting values of 0 or 1.0, and its

Table 5. *T*-Dependent $[\theta]_{222} - [\theta]_{208}$ Slopes for Ala_4Lys Oligomers and polyAlanines

solvent	*T* range °C	slope *B*	$100\sigma_{Linear}/\langle[\theta]\rangle_{222}$	slope range	$\frac{1}{B}\left\langle\frac{\Delta B(T)}{\Delta T}\right\rangle 10^3$/°C	CC
			I. $AcHel(Ala_4Lys)_4Ala_2NH_2$			
water−EG	−20−60	2.42	−3.6	1.53−3.60	−13.2	−0.993
water−EG	5−60	2.00	−2.3	1.53−2.66	−14.0	−0.998
water−ClO_4^-	5−60	1.87	−2.5	1.53−2.23	−9.9	−0.984
water−TFE	5−60	1.85	−1.3	1.41−2.26	−12.3	−0.990
			II. $^+H_2(Ala_4Lys)_4Ala_2NH_2$			
water−EG	−20−60	1.51	−3.5	1.12−1.94	−8.3	−0.98
water−EG	5−60	2.00	−2.3	1.12−1.57	−9.0	−0.94
water−ClO_4^-	5−60	1.87	−2.5	1.08−1.55	−8.3	−0.99
water−TFE	5−60	1.42	−1.2	1.19−1.71	−8.1	−0.99
			III. uncapped and capped polyalanines in water			
Ala_{28}	5−60	1.70	−2.3	1.39−2.07	−9.4	−0.98
Ala_{19}	5−60	1.54	−3.0	1.24−1.86	−8.2	−0.89
Ala_{16}	5−60	(1.1)	−5.0	0.30−1.44	(−24)	−0.96
$Ac^{\beta}DHelA_8\beta a$	5−60	2.46	−2.1	1.99−2.91	−12.7	−0.90

[a] Full structure: Ac-$^{\beta}$Asp-Hel-$A_8\beta InpK_2W$-NH_2; in which β is β-aminoalanine.

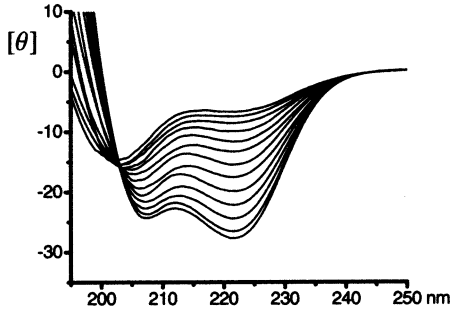

Figure 13. Temperature-dependent CD manifolds in water from 5 to 60 °C for spaced solubilized A_{19}. Spectra were measured at 5 °C intervals; at 222 nm from top to bottom, spectra appear in order of decreasing temperatures. Ellipticity units: 10^3 deg cm^2 dmol^{-1}.

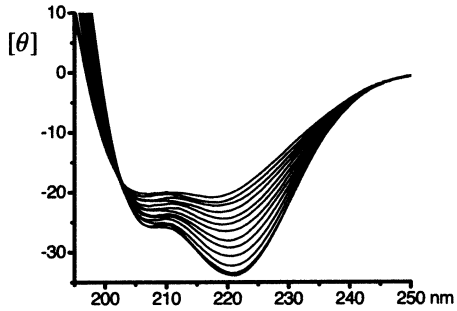

Figure 14. Temperature-dependent CD manifolds in water from 5 to 60 °C for $^{\beta}AspHelAla_8\beta InpK_2W$. Spectra were measured at 5 °C intervals; at 222 nm from top to bottom, spectra appear in order of decreasing temperatures. Ellipticity units: 10^3 deg cm^2 dmol^{-1} Helix stabilizing properties for the N-cap βAspHel and the C-cap β, β-aminoalanine, have been previously reported.[56,57]

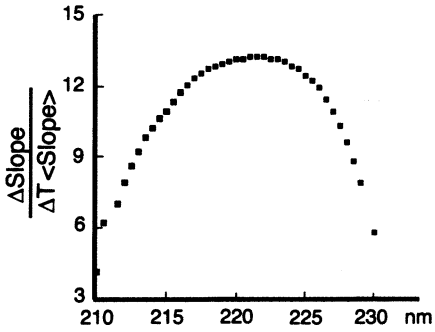

Figure 15. Analysis of the CD manifold of Figure 8 for $AcHel(Ala_4Lys)_4Ala_2NH_2$ in 16 mol % EG−water at 60 to −20 °C. A plot of wavelength dependence of the curvature expressed as the relative mean temperature-dependence of local slopes of parametric correlations of $[\theta]_\lambda$ vs $[\theta]_\lambda$ for $210 < \lambda < 230$. Ordinate units are 10^3 K^{-1}.

temperature dependence, which underlies the correlation of local parametric slope with temperature, is expected to drop dramatically.

For the spaced, solubilized A_n series, CD manifolds were measured for A_{28}, A_{19}, and A_{16} in water at temperature intervals of 5 °C. Our previous analysis[9] allows tentative assignment of the following fractional helicities near 0 °C: A_{28}, FH ∼ 0.75; A_{19}, FH ∼ 0.65; A_{16}, FH ∼ 0.45. For the two highly helical peptides A_{28} and A_{19}, the slopes *B* and the slope ranges vary inversely with these FH values, as expected.[58] Near 0 °C or below, the A_n peptides of Table 5 with intense $[\theta]_{222}$ values that exceed literature standards are A_{28} and $Ac^{\beta}AspHel$-$A_8\beta InpK_2WNH_2$, studied in water. In dilute salt with or without EG or TFE-additives, $AcHel(Ala_4Lys)_4Ala_2NH_2$ also meets this condition. The CD manifolds of all these peptides yield maximum values for *B* and for the relative curvature parameter of column six of Table 5. Notably, for its short length the polyalanine peptide $Ac^{\beta}AspHelA_8\beta InpK_2WNH_2$, Figure 14, exhibits exceptional 222 nm ellipticity at low temperatures. As we have reported elsewhere,[55c] the A_8 sequence defines the helical region of this peptide that contributes significantly to the intensity of $[\theta]_{222}$. This example demonstrates that for short helical peptides, very efficient helix stabilizing caps can induce exceptional CD intensity and parametric curvature.

The question remaining among those posed at the start of this section concerns the wavelength region within which the parametric curvature effect is maximal. It can be addressed by a parametric wavelength scan. For the $AcHel(Ala_4Lys)_4Ala_2NH_2$ helical manifold, Figure 10B, parametric correlations of $[\theta]_\lambda$ vs $[\theta]_{208}$ were carried out over the 210 to 230 nm wavelength region in which data yielded acceptable CC values (−0.90 to −1.0). Figure 15 shows the wavelength dependence of the

(56) Deechongkit, S.; Kennedy, R. J.; Tsang, K.-Y.; Renold, P.; Kemp, D. S. *Tetrahedron Lett.* **2000**, *41*, 9670−9683.
(57) Maison, W.; Arce, E.; Renold, P.; Kennedy, R. J.; Kemp, D. S. *J. Am. Chem. Soc.* **2001**, *42*, 10 245−10 254.
(58) The anomalous values for A_{16}, found in columns 4, 5, 6 almost certainly reflect the very low FH values for this peptide at temperatures above 40 °C. In this region, slope is strongly dependent on $[\theta]_U$ values, and FH probably shows a diminished dependence on temperature.

relative curvature variable of Table 5, column 6. The region of maximum relative curvature is clearly centered at 222 nm, but curvature above the limit of likely measurement error is seen within a ca. 20 nm region. This analysis was also applied to other highly helical peptides of Table 5 (data not shown); all showed maximum relative temperature-dependent curvature near 222 nm, but measurement errors limited the precision with which the curvature envelope in neighboring regions could be defined. The form of Figure 15 suggests that the curvature anomaly is associated with a relative increase with decreasing temperature of the rotatory strength of the n−π* CD transition, referenced to any change in the strength of the $\pi-\pi$* transition.

The simplest explanation is a temperature dependence of the ellipticity $[\theta]_H$ for the completely α-helical conformation. A definitive test requires demonstration of experimentally separable temperature-induced changes in $[\theta]_{Exp}$, attributable either to an increase in FH or to an intrinsic temperature dependence of $[\theta]_H$. Unfortunately accurate CD-independent FH assignments over a wide temperature range are currently unavailable. The alternative requires a demonstration of conditions in which $[\theta]_{exp}$ can be plausibly argued to approximate $[\theta]_H$. The CD manifold of Figure 10C for the peptide AcHel$(Ala_4Lys)_4Ala_2NH_2$ appears to provide this alternative. This manifold was constructed by extending the accessible low-temperature limit of Figure 10B from −20 to −50 °C by increasing the EG concentration to 32 mol %.

In this manifold $[\theta]_{208}$ converges to a low-temperature limit of −44 000 deg cm^2-dmol^{-1} at ca. −20 °C, remaining constant at lower temperatures, as do ellipticities in the 200−210 nm and 230−250 nm regions. Within experimental error, only ellipticities in the region 210−230 nm increase in intensity with decreasing temperature, and a difference spectrum obtained by subtracting the CD at −20 °C from that at −50 °C resemble a Gaussian curve centered at 222 nm. The slope *B* of a parametric $[\theta]_{222}$ vs $[\theta]_{208}$ plot thus assumes very large values in the region −20 to −50 °C, suggesting that FH has attained a maximal value and is independent of temperature below −20 °C. The increased intensity of $[\theta]_{222}$ at these temperatures is plausibly interpreted as reflecting a temperature-dependent change in the CD spectrum of a conformational ensemble of a maximally helical peptide that occurs in a local wavelength region. This change is not small: −64 200 to −56 000 deg cm^2 dmol^{-1} over 30 °C temperature change, and it shows a roughly constant dependence on temperature in this region of 260 deg cm^2 K^{-1}dmol^{-1}. The possible structural changes consistent with such a temperature dependence are discussed in the following section.

Throughout this analysis, we have assumed that the addition of ethylene glycol EG to the aqueous media used to measure temperature-dependent CD spectra for AcHel$(Ala_4Lys)_4Ala_2NH_2$ and related peptides can be viewed as a perturbation. Given the importance of the above comparisons and analyses for the resolution of the parametric curvature problem and the key role that low-temperature studies play in these analyses, it is appropriate to revisit this issue by considering the effect of aqueous solvent changes on $[\theta]_{222}$ for the simple and N-capped $(Ala_4Lys)_4Ala_2NH_2$ peptides.

We initiated aqueous studies of these peptides by selecting 0.2 M perchlorate-water for studying CD manifolds in the range of 0 to 60 °C and aqueous 5 M NaCl (brine) for studies conducted below 0 °C. Two more test solvents were generated by adding to the dilute salt solution either 16 mol % EG or 16 mol % TFE.

In brine an 80% decrease in $[\theta]_{222}$ intensity is seen for AcHel$(Ala_4Lys)_4Ala_2NH_2$ as the temperature is raised from 0 to 60 °C. In TFE-water the corresponding change is only 40%, and nearly the same changes with temperature are seen in these solvents for $(Ala_4Lys)_4Ala_2NH_2$. This temperature variation in water and EG-water results respectively in 70 and 55% $[\theta]_{222}$ changes for the N-capped peptide, and in 79% and 71% changes for the simple peptide. Near 0 °C in water and EG-water this peptide shows nearly identical values of $[\theta]_{222}$, implying that EG significantly stabilizes helices at high temperatures, but the effect becomes insignificant as the temperature is lowered to room temperature and below, as is evident from comparisons of Figures 11A & 11C. This result is consistent with reported effects of dilute EG on the stabilities of globular proteins.[59]

CD measurements were carried out at −20 °C on AcHel$(Ala_4Lys)_4Ala_2NH_2$ in both 16 mol % EG and 5 M brine, and these demonstrated nearly identical $[\theta]_{222}$ values. Unfortunately the opacity of brine at short UV wavelengths rendered it useless as a solvent for parametric wavelength correlations.

As seen in Figure 12, parametric correlations allow comparisons of properties of temperature-dependent CD manifolds measured for a helical peptide in a series of solvents or for a series of structurally related peptides. A parametric dual wavelength plot of CD data from a manifold generates a signature, defined by a locus of data points within $[\theta]_{222}$—$[\theta]_{208}$ space. The relative proximity of two or more such signatures in that space provides a measure of the similarity of their corresponding CD manifolds. Figure 12 compares six parametric $[\theta]_{222}$ vs $[\theta]_{208}$ signatures of CD manifolds derived from N-capped AcHel$(Ala_4Lys)_4Ala_2NH_2$ in water, EG-water, and TFE-water; free $(Ala_4Lys)_4Ala_2NH_2$ in water and EG-water; and spaced, solubilized A_{19} in water.

To a reasonable approximation the locus of the manifold for AcHel$(Ala_4Lys)_4Ala_2NH_2$ in water (filled circles) can be seen as extending the locus of the manifold for $(Ala_4Lys)_4Ala_2NH_2$ in water (open circles) into a more intense ellipticity region. A similar extension is seen for the corresponding locus pair for manifolds measured in EG-water (filled and open squares). This feature is expected if, as noted earlier in this discussion, the AcHel cap primarily serves to stabilize a helical peptide without changing its CD properties.

Three of the regions of $[\theta]_{222}$—$[\theta]_{208}$ space shown in Figure 12 are defined by CD manifolds of peptides that lack the N-cap, and significantly they are nearly contiguous. The locus defined by open triangles corresponds to the manifold for the A_{19} peptide in water, and it approximates the region defined by the locus pair observed for $(Ala_4Lys)_4Ala_2NH_2$ in water and in EG-water. Although the latter peptide contains 22 amino acid residues and thus might be expected to exhibit more intense residue ellipticities, at the pH of the study it bears a helix-destabilizing positive charge at its N-terminus, and incompletely screened repulsions between charges on the four Lys residues may result in additional destabilization. Notably the locus of the manifold for $(Ala_4Lys)_4Ala_2NH_2$ in EG-water is bounded by those for the manifolds measured in water alone. For the CD manifolds of these peptides at 0−60 °C the addition of EG to water thus constitutes a small CD perturbation.

(59) Timasheff, S. N.; Inoue, H. *Biochemistry* **1968**, *7*, 2501−2513.

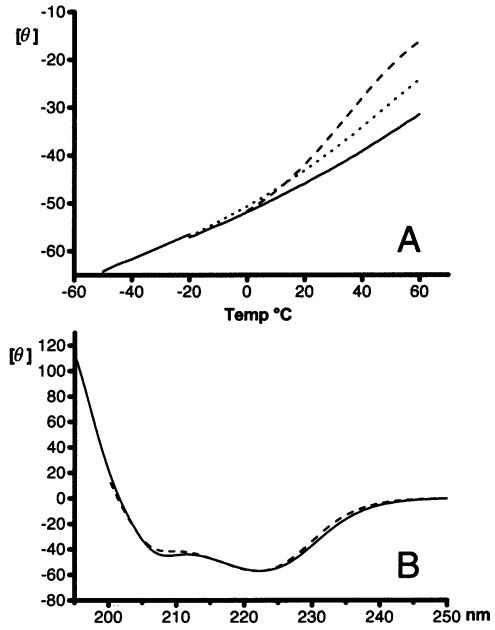

Figure 16. A. Temperature dependence of $[\theta]_{222}$ for AcHel(Ala_4-$Lys)_4Ala_2NH_2$ in aqueous perchlorate alone (dashed line); with added 16 mol % EG (dotted line); with added 32 mol % EG (solid line). B. CD spectra of AcHel($Ala_4Lys)_4Ala_2NH_2$ in 0.2 M aqueous perchlorate with added 16 mol % EG (dotted line); with 32 mol % EG (solid line). EG = ethylene glycol. $T = -20$ °C.

The CD manifolds of Figure 10 were measured in aqueous solution through the addition of 16 or 32 mol % EG. Do their properties at least qualitatively correspond to those of CD manifolds measured in water? Can one exclude EG as a primary source of the unusual properties of low-temperature CD spectra of these manifolds? This key issue is addressed by the analyses of Figure 16A and spectra of Figure 16B. The former show that in dilute aqueous salt the temperature dependences of the intensities of $[\theta]_{222}$ for AcHel($Ala_4Lys)_4Ala_2NH_2$ in the absence and presence of 16 and 32 mol % EG approximate a simple linear form and converge to a common limit at 0 °C. Moreover, lowering the temperatures of the two EG-water mixtures extends the region of accurate linear extrapolation into the −20 to −50 °C range within which the manifold of Figure 10C was measured. The CD spectra of Figure 16B, measured at −20 °C in the two EG-water mixtures, are essentially superimposable.[60] Under these conditions, the concentration of EG clearly can be varied over wide limits without detectable effects on the CD spectra of this peptide archetype. By the simplest interpretation of these findings, the water additive EG permits low temperature CD studies in aqueous media but minimally perturbs the CD-relevant properties of water.

Inspection of Figure 12 shows that the locus of the CD manifold for AcHel($Ala_4Lys)_4Ala_2NH_2$, measured in 16 mol % TFE-water is isolated from any other locus of the study, and comparison of the details of the CD manifolds of Figure 11E and F with the manifolds of Figure 11C and D reveals large TFE-induced anomalies. Figure 11E and F reflect strong helix stabilization, but the large values of R_2 observed for other stabilized peptide helices of this study are not seen in TFE-water mixtures.

First introduced by Goodman and co-workers,[61] TFE is widely employed as an exceptionally efficient helix-enhancing water additive.[12a,51] In the concentration range of this study, helicity enhancement has been attributed to a dramatic change in the hydrogen bonding capacity of water that results in a selective stabilization of internally hydrogen bonded peptide conformations, such as helices.[62] A comparison of the CD manifolds of Figure 11C and E shows that at 60 °C for the N-capped peptide, addition of TFE to water increases intensities of both $[\theta]_{208}$ and $[\theta]_{222}$ by 95%. At 5 °C, TFE addition results in a mere 22% increase in intensity of $[\theta]_{208}$ and decreases that of $[\theta]_{222}$ by 6%. Overall effects of adding TFE include an unprecedented decrease in the temperature sensitivity of CD ellipticities at both 208 and 222 nm and at ca. 5 °C a nearly 30% increase of the intensity of $[\theta]_{208}$ relative to that of $[\theta]_{222}$. Similar though smaller effects are observed for the CD manifolds of the uncapped peptide.

Are the structures of α-helices formed by AcHel(Ala_4-$Lys)_4Ala_2NH_2$ in water or EG-water significantly different from those formed in 16 mol % TFE? This question can only be addressed by differential NMR structural analyses of peptide archetypes in water and TFE-water mixtures. Until such results are available, our present findings imply that peptide helices formed in water-TFE mixtures are inappropriate models for helices formed in more typical aqueous solutions.

Discussion

The foregoing analysis has established that curvature of parametric ellipticity plots of data from temperature-dependent CD manifolds is the rare exception for most literature peptides but is the rule for alanine-rich helices. For these the region of anomalous curvature is centered at the 222 nm ellipticity minimum, and a highly helical peptide at temperatures below −20 °C shows CD spectra that are temperature independent at most wavelengths, but not in the region centered at 222 nm. This result tentatively suggests that with the exception of a ca. 15 nm region centered at 222 nm, where it is strongly temperature dependent, the residue ellipticity of a completely helical alanine-rich peptide $[\theta]_H$ may be nearly independent of temperature.

Given appropriate model spectra, CD is a tool of unique ease and power for assigning peptide conformations. Without models, CD is ineffectual.[63] Until appropriate models become available, we cannot assign structures that account for the anomalous features of the CD spectra of our alanine-rich helical archetypes. The available evidence does justify rejection of some classes of structural interpretations. It also points toward viable alternatives, together with experiments that might test them.

Could one plausibly assign the CD spectra shown in Figure 10C for AcHel($Ala_4Lys)_4Ala_2NH_2$ at temperatures below −20 °C to a conformational equilibration between highly helical and structured nonhelical states? On two counts, we think not. First, among the range of CD ellipticities exhibited by the amide functions of the peptide backbone in the 210−230 nm region, those of helices are uniquely intense.[1c] Introduced forty years ago,[64] the theory underlying peptide CD spectra has achieved

(60) As seen in Figure 16, the $[\theta]$ values in 16 and 32 mol % EG are −41.6 and −43.6 for the 208 nm minimum, and −57.0 and −56.5 for the 222 nm minimum (units of 10^3 deg cm^2 dmol^{-1}, suggesting that the effect of this solvent change on $[\theta]$ may be modest.

(61) Goodman, M.; Listowsky, I.; Masuda, Y.; Boardman, F. *Biopolymers* **1963**, *1*, 33−42.
(62) Cammers-Goodwin, A.; Allen, T. J.; Oslick, S. L.; McClure, K.; Lee, J.; Kemp, D. S. *J. Am. Chem. Soc.* **1996**, *118*, 3082−3090.
(63) Ovchinnikov, Yu. A.; Ivanov, V. T., *Tetrahedron* **1975**, *31*, 2177−2209.

maturity, and for the first time it can be used to model the rotatory strength of proteins from the X-ray crystallographic database accurately throughout the 190−250 nm region.[37,65] The contribution to rotatory strength by amides of a particular peptide chromophore depends on proximity-induced coupling between its amide n−π^* and $\pi-\pi^*$ electric and magnetic dipole transitions, and the intensity of this contribution is strongly dependent on the particular regions of ϕ, ψ space that are populated by the neighboring residues. Peptide helices provide a combination of these factors that results in unusually high rotatory strength. Because the CD properties of most populated regions of Ramachandran space have been explored experimentally by analysis of rigid peptide models, it seems unlikely that any previously uncharacterized nonhelical conformation could match helical rotatory strength in the region of 210 to 230 nm.

NMR evidence provides a second argument against the presence of nonhelical structured states within highly helical alanine-rich peptides. Largely owing to the compactness of helical conformations and the resulting wealth of short van der Waals interactions that they generate, modern NMR spectroscopy is a powerful structural tool for characterizing helices. A first report of a ^{1}H NMR NOESY analysis of an alanine-rich highly helical peptide with anomalously intense $[\theta]_{222}$ only revealed local interactions characteristic of an α-helix.[66] Two recent, more definitive NMR studies on alanine-rich peptides mapped conformational properties throughout the peptide backbone for typical alanine-rich peptides of medium length. The first used solution-phase 750 MHz ^{1}H 2D NOESY spectroscopy.[67] The second applied the 2D MAS solid-state spectroscopic method to a ^{13}C and ^{15}N-labeled alanine-rich peptide in a glycerol-water glass at −140 °C.[68] Both studies established the presence throughout the peptide sequences of the expected helical NOE interactions and no others. However, in addition to NOE signatures characteristic of α helices, both found 3_{10} helical signatures, particularly at the peptide end regions.

Could a temperature-dependent equilibration between α and 3_{10} helical conformations account for our parametric CD curvature anomalies? First characterized by Millhauser and coworkers using a double spin label technique,[69] 3_{10} helical content has been demonstrated in a variety of peptides, particularly at helix ends and within short to medium length alanine-rich sequences. From NMR evidence, these conformations are certainly present, but it is difficult to see how our CD anomalies can be explained by a low-temperature α-3_{10} equilibration because 3_{10} structures are expected to reduce the intensity of $[\theta]_{222}$ relative to other ellipticities in the 208 to 230 nm region. Most literature models demonstrate that R_2 for a 3_{10} helix is substantially less than 1.0.[70,71]

The most plausible explanation for our observations is a structural variability of the α-helix itself. This variability must meet three conditions in order to explain our low-temperature CD findings. First, an α-helical conformation is favored at low temperatures and exhibits the unusually intense ellipticities in the 210−230 nm region seen in Figure 10C. Second, evidence must be provided that conformers of α-helices can change significantly in relative abundance at low temperatures. Third, alanine-rich peptides must be shown to be unusually likely to undergo these conformational changes. Literature precedents in fact exist for the second and third of these conditions.

The unusual structural variability of α-helices was demonstrated thirty years ago and has played an ongoing, subordinate role in subsequent analyses of helical structure. In 1967, study of the X-ray structure of hen egg white lysosome led Nemethy et al[72] to define the hydrophilic α_{II} helix, which retains the 3.6_{13} hydrogen bonding signature of the classical Pauling α-helix, but differs from it in the large outward tilt of its backbone amide planes. This tilt results in longer and presumably weaker amide-amide hydrogen bonds and greater solvent accessibility for the lone pairs of amide oxygens. In 1972, Parrish and Blout[73] reported that polyalanine, which is insoluble in common CD solvents, could be dissolved in hexafluoro-2-propanol HFIP, which is strongly interacting and helix-stabilizing. Helices were demonstrated in these solutions by a number of physical methods, but the CD spectra were markedly unlike those of other helical homooligopeptides.[74] Moreover, upon dilution with water the CD spectrum of polyalanine became conventionally helical. Similar behavior was observed for alanine-rich oligopeptides, and Parrish and Blout proposed that in HFIP, these peptides form a "doubly bonded" helix similar to the α_{II} conformation, with carbonyl oxygens hydrogen bonded both to solvent and to amide NH functions. These workers noted that alanine-rich peptides appear to be unusually susceptible to this type of structural ambiguity.

In 1989, with the aim of characterizing the anomalously weak helical CD signature of bacteriorhodopsin, Gibson and Cassim[75] measured CD spectra of the native protein in both oriented and randomized films. Citing a precedent for their results in the study of Parrish and Blout, they found that for their CD spectra of oriented films, the α_{II} helical conformation provided the best explanation for intensity of the ellipticity band centered at 222 nm and the dependence of its intensity on sample orientation. They also noted consistency between their observations and calculations of Manning and Woody[76] which demonstrate a strong decrease in intensity of the CD helical $\pi-\pi^*$ transition if the α_I conformation is changed to α_{II}. Independent support for their assignment had been provided earlier by Krimm and Dwivedi, based on an infrared study of the amide I and amide

(64) Woody, R. W.; Tinoco, I. *J. Chem. Phys.* **1967**, *46*, 4927−4945. Bayley, P. M.; Nielsen, E. B.; Schellman, J. A. *J. Phys. Chem.* **1969**, *73*, 228−243. Woody, R. W. *J. Chem. Phys.* **1968**, *49*, 4797−4905.
(65) (a) Hirst, J. D.; Besley, N. A. *J. Chem. Phys.* **1999**, *111*, 2846−2847. (b) Woody, R. W.; Sreerama, N. *J. Chem. Phys.* **1999**, *111*, 2844−2845. (c) Hirst, J. D. *J. Chem. Phys.* **1998**. *109*, 782−788.
(66) Lockhart, D. J.; Kim, P. S. *Science* **1993**, *260*, 198−202.
(67) Millhauser, G. L.; Stenland, C. J.; Hanson, P.; Bolin, K. A.; van de Ven, F. J. M. *J. Mol. Biol*. **1997**, *267*, 963−974.
(68) Long, H. W.; Tycko, R. *J. Am. Chem. Soc.* **1998**, *120*, 7039−7048.
(69) (a) Miick, S. M.; Martinez, G. V.; Fiori, W. R.; Todd, A. P.; Millhauser, G. L. *Nature* **1992**, *359*, 653−655. (b) Fiori, W. R.; Miick, S. M.; Millhauser, G. L. *Biochemistry* **1993**, *32*, 11 957−11 962. (c) Bolin, K. A.; Milhauser, G. L. *Acc. Chem. Res.* **1999**, *32*, 1027−1033.
(70) Toniolo, C.; Polese, A.; Formaggio, F.; Crisma, M.; Kamphuis, J. *J. Am. Chem. Soc.* **1996**, *118*, 2744−2745.
(71) This assignment is not without its critics; see: Andersen, N. H.; Liu, Z.; Prickett, K. S. *FEBS Lett.* **1996**, *399*, 4752.
(72) Nemethy, G.; Phillips, D. C.; Leach, S. J.; Scheraga, H. A. *Nature* **1967**, *214*, 363−365.
(73) Parrish, J. R., Jr.; Blout, E. R. *Biopolymers* **1972**, *11*, 1001−1020.
(74) Johnson, W. C., Jr.; Tinoco, I., Jr. *J. Am. Chem. Soc.* **1972**, *94*, 4389−4399.
(75) Gibson, N. J.; Cassim, J. Y. *Biochemistry* **1989**, *28*, 2134−2139.
(76) Manning, M. C.; Woody, R. W. *Biopolymers* **1987**, *26*, 1731−1752; Manning, M. C.; Woody, R. W. *Biopolymers* **1991**, *31*, 569−586.

A bands of this protein.[77] Equilibration between these conformations has been proposed to play a functional role within this membrane-bound protein, and switching between α_I and α_{II} conformations for the helices of this protein upon light absorption is under active investigation.[78]

Are α_I and α_{II} the unique α-helical conformations? In 1968, Ramachandran and Sasisekharan reported that ϕ, ψ values for the α_I and α_{II} conformers define the approximate outer limits for an extended region of conformational space that is compatible with α-helices.[79] In support of their calculations, recent molecular modeling of the solvent dependence of helical conformations of short Ala_n sequences confirms the presence in Ramachandran space of a free energy trough defined by $\phi + \psi = -107°$. Within this trough, a series of conformations retain the 3.6_{13} hydrogen bonding signature of an α-helix, but backbone amide residues undergo varying degrees of tilt with respect to the helix axis, with resulting changes in the helix radius. Although the trough contains shallow local minima, it is characterized by a soft energetic deformation mode.[80]

Evidence from the globular crystal structures of the Protein Data Bank provides independent confirmation of these modeling results. Drawing upon a 29-protein database, Besley and Hirst[37] noted that a graph of ϕ vs ψ for the helical α-carbons within this data set results in a typical diffusely populated ellipsoidal region with long axis oriented at roughly 45° within a rectangle defined as $-25° > \phi > -95°$ and $-10° > \psi > -80°$. However, if these ϕ, ψ values are averaged for each helix that appears within the data set, and the averages are replotted, in accord with previous modeling results a reasonable fit to a line defined by $\phi + \psi = -107°$ is obtained. This result suggests that the proteins of the database contain a diverse structural range of α-helices. Only about 10% of these ϕ, ψ values lie close to the classic Pauling-Corey limit ($\phi = -48°$, $\psi = -58°$), 20% lie close to the range reported for a fiber diffraction study of polyalanine[81] (−58°, −48°), but nearly 50% lie close to values of (−64°, −36°) typical of PDB proteins. About 20% lie close to the α_{II} structure (−80°, −27°). These examples correspond to helices found in a structural database composed of crystalline globular proteins, which may not be typical for broader protein classes.

These precedents do not provide an example of a helical peptide that shares the anomalous CD properties that we have observed for alanine-rich peptides. Dang and Hirst have recently suggested that these properties may be consistent with helices that contain exceptionally short amide-amide hydrogen bonds.[54] Though currently lacking precedent in the X-ray protein database, this intriguing proposal clearly merits scrutiny and testing. A recent study of Fasman[82a] may provide evidence for the biological relevance of CD spectra of our alanine-rich peptides. Given CD spectra and X-ray structure-derived percentages of each type of secondary structure within each of a series of PDB proteins, deconvolutions yield limiting CD spectra for helices, sheets, turns, and other elements of local peptide conformation.[1c] Fasman and co-workers have developed an alternative, convex constraint analysis CCA,[82b] that does not rely on X-ray crystallographic data and thus can be applied to proteins that do not crystallize and are not represented within the PDB. When CCA is applied to globular proteins, it predicts a single helical CD basis spectrum that is unexceptional.[31] When it is applied to the CD manifold composed of spectra measured in mild aqueous detergents for a data set comprising 30 membrane-bound proteins, two distinct deconvoluted helical CD curves were observed. The α-curve is again unexceptional and corresponds to helices characteristic of normal protein domains. The α_T curve is assigned to transmembrane helices and is characterized a positive red-shifted band in the range 195−200 nm ($[\theta] + 95\,000$ deg cm^2 dmol^{-1}), a negative band at 208 nm ($[\theta]$ −50 000 deg cm^2 dmol^{-1}), and a second negative band at 222 nm ($[\theta]$ −60 000 deg cm^2 dmol^{-1}). Above 210 nm the deconvoluted α_T-curve correlates within 5% with low-temperature CD curves reported in Figure 10C for AcHel$(Ala_4$-$Lys)_4Ala_2NH_2$. Though suggestive, this correlation awaits independent structural confirmation. As pointed out by a referee, the convex constraint analysis can result in spurious correlations if, for a given protein database, too many basis spectra have been selected.

What has been clearly established at this preliminary stage in the parametric analysis of temperature-dependent CD manifolds? It is clear that for most protein-derived helical peptide sequences, linear correlations are the rule, and literature correlations of FH with $[\theta]_{222}$ are almost certainly accurate. We have also shown that a polyalanine sequence or an alanine-rich sequence that contains residues such as Arg, Lys, or Glu is a sufficient precondition for the presence of parametric curvature. Is an alanine-dominated sequence also a necessary precondition for curvature? In other words, by selecting a subset of natural amino acids other than alanine, can one find peptide sequences that frequently show parametric curvature? The CD properties of the peptide sequence studied by Kuhlman et al.[40] suggest this possibility. This sequence, with curvature listed in Table 2, lacks amino acid residues with β-branched or aromatic side chains. CD curvature tests of helical peptides constructed from the amino acids found in the Kuhlman peptide and studies of polyalanine hosts containing β-branched guests are obvious first steps in an exploration of this important issue. Alanine-rich peptides may prove to be only the simplest examples of a broader class of helical peptides whose members exhibit curvature.

Medium-sized polyalanines, alanine-rich peptides, or other helically disposed peptides that bear pairs of recently introduced helix-stabilizing peptide N and C-capping functions are likely to approach 100% helicity at moderate to low temperatures in water and other aqueous solvents.[55c,57] Protection factor measurements allow experimental confirmation of their helicities, and such peptides thus provide obvious choices for CD calibration standards. Temperature-dependent CD measurements on a series of such calibrated peptides that span a significant range of lengths can address the following questions: (1) What is the dependence of limiting CD ellipticity on measurement temperature, solvent, and length of the helical region? (2) Do single site amino acid substitutions, for example by β-branched amino acids, dramatically change these spectra and temperature dependences to those expected for normal peptides? (3) For

(77) Krimm, S.; Dwivedi, A. M. *Science* **1982**, *216*, 407−408.
(78) (a) Torres, J.; Sepulcre, F.; Padros, E. *Biochemistry* **1995**, *34*, 16 320−16 326. (b) Wang, J.; El-Sayed, M. A. *Biophys. J.* **2000**, *78*, 2031−2036.
(79) Ramachandran, G. N.; Sasisekharan, V. *Adv. Protein Chem.* **1968**, *23*, 284−438.
(80) Mahadevan, J.; Lee, K.-H.; Kuczera, K. *J. Phys Chem. B* **2001**, *105*, 1863−1876.
(81) Arnott, S.; Dover, S. D. *J. Mol. Biol.* **1967**, *30*, 209−212.
(82) (a) Fasman, G. D. *Biopolymers* **1995**, *37*, 339−362. (b) Perczel, A.; Park, K.; Fasman, G. D. *Anal. Biochem.* **1992**, *203*, 83−93.

these peptides can a simple temperature-dependent equation allow accurate correlation of FH with $[\theta]_{exp,222}$?

Answers to these questions will not define the structural differences between helical peptides that exhibit normal and anomalous CD spectra, but provided highly stabilized N and C-capped peptides become available, X-ray crystallography combined with solution and solid state NMR methods may be able to do so. These should provide the CD standards for anomalous helical spectra that are currently lacking. The ellipticity minimum at 222 nm has many advantages as a helicity standard.[7] From a rigorous recalibration of the temperature dependences of $[\theta]_{222}$ values[83,84,85] it should be possible to reestablish CD as the simplest and most efficient tool for quantifying peptide helicity.

Summary

For any peptide that exhibits an additive or temperature-dependent manifold of CD spectra with an isodichroic point at 203 nm, fractional helicity is conventionally calculated as proportional to the value of $[\theta]_{222}$. In this report, we have demonstrated that for alanine-rich peptides the presence of an isodichroic point near 203 nm does not ensure high precision for FH calculations based on $[\theta]_{222}$ values. We have introduced a more rigorous precondition for any precise calculation of FH. A parametric plot of residue ellipticities $[\theta]_{222}$ and $[\theta]_{208}$ taken from the manifold must be linear over the additive or temperature range of the proposed study.

We have applied this test to a literature database of CD spectra obtained for proteins or protein-derived peptides and found that nearly all meet this linearity condition. For these, conventional CD-based calculations of FH are likely to be accurate. When applied to helical polyalanines or alanine-rich peptides, the parametric $[\theta]$ correlation almost invariably demonstrates concave upward curvature, and low-temperature studies of alanine-rich peptides suggest origin in anomalous temperature dependence for $[\theta]_H$ that is maximal at 222 nm. On the basis of literature precedents a temperature-dependent equilibration between conformers of α-helices that differ in ϕ, ψ angles is suggested.

Appendix: Form of CD Manifolds of Helical Peptides near 203 nm; Significance of the Isodichroic Point. This appendix focuses on the properties of isodichroic points that may appear in CD manifolds for peptide and protein helices that are constructed by varying progress variables such as temperature or denaturant concentration. The appearance of an isodichroic point near 203 nm in data-rich manifolds such as those of Figures 2 and 10A,B provides a visually compelling image for a simple two-state peptide FH model. At a glance, it appears to validate assignment of quantitative FH values from CD data. How sensitive is the dichroic point to deviations from two-state behavior, how valid is this FH assignment, and what is the predictive significance of the frequently observed consistency seen for the wavelength and ellipticity of this isodichroic point? A brief review of helical CD manifolds provides a useful foundation for addressing these questions.

A sequence of CD spectra that monitor the melting of a helical globular protein of compact native structure defines the gold standard for helical manifolds. The protein unfolds cooperatively in solution over a narrow temperature range, and only native and unstructured states are present at significant concentrations.[6] The residue ellipticity $[\theta]_H$ of the native state exhibits little or no temperature dependence, and the experimental residue ellipticity $[\theta]_{Exp}$ thus corresponds to a linear function of the constants $[\theta]_H$ and $[\theta]_U$, eq 1. The composition of the unstructured state is heterogeneous and temperature dependent,[5b,14] implying a corresponding temperature dependence for $[\theta]_U$. However, at temperatures within or below the melting range and at wavelengths greater than 210 nm, where $[\theta]_H$ is more intense than $[\theta]_U$, the effect of this temperature dependence is slight. It does assume significance in the wavelength region of the experimental isodichroic point, and thus must limit the precision of isodichroic behavior, particularly if the temperature range of the manifold corresponds to a large variation in FH.

At a molecular level, the melting or denaturation of helically disposed simple peptides is not a two-state process, and the interpretation of isodichroic points that appear in the corresponding CD manifolds is more complex. The folding transition between fully and partially helical conformers and unstructured conformers is gradual, and for feasible changes in the progress variable, the transition is almost invariably incomplete. Because the helical properties of the peptide cannot be modeled as involving a single helical molecule, χ_H is not a useful measure of helicity, but can be replaced by CD-monitored FH, averaged over the range of all conformers. A basic assumption in any two-state model is an invariance of the residue ellipticity contributed by the flanking amide residues of each single helical α-carbon to helix length or structure.[13] The experimental $[\theta]$ is an average over a range of different conformations and thus both $[\theta]_U$ and $[\theta]_H$ are expected to be dependent on temperature or other progress variables.

To address the initial questions of this Appendix, we introduce a simple model for an isodichroic point by assuming its lack of precision can be attributed to monotonic dependences of $[\theta]_H$ and $[\theta]_U$ on a progress variable like temperature. Between 195 and 210 nm, experiment and theory confirm that $[\theta]_H$ decreases steeply and nearly linearly from a positive maximum near 192 nm to a negative minimum at 208 nm. Consistent with both theory[86] and experiment[87] we model a temperature dependence of $[\theta]_H$ by proportionally reducing the intensities of both maximum and minimum, and that of $[\theta]_U$ by a linear function spanning a negative temperature dependent minimum slightly below 200 nm to a negative, nearly temperature-independent value in the range of 205 to 209 nm (see Figure 5). At the wavelength of the isodichroic point, these lines cross and $[\theta]_H$ equals $[\theta]_U$. Relative to $[\theta]_H$, $[\theta]_U$ in this region varies only moderately with wavelength and is consistently negative, but $[\theta]_H$ decreases steeply from a large positive to a large negative

(83) Although we question the experimental basis of their assignments, temperature-dependent $[\theta]_{222}$ values have been previously reported by Luo and Baldwin[52] as well as Scholtz, J. M.; Qian, H.; York, E. J.; Steward, J. M.; Baldwin, R. L. *Biopolymers* **1991**, *31*, 1463−1471.

(84) In ref 83, temperature dependence of $[\theta]_{H,\ 222}$ was estimated from CD properties of dimeric helical coiled coils. Holtzer et al. have questioned the validity of this assignment.[85] In ref 52 extrapolation from CD properties of solutions containing high concentrations of TFE were used to define the temperature dependence of $[\theta]_{H,222}$. Our own studies of TFE-induced helicity (e g., Figures 11E, F, and 12) suggest that undefined solvent effects introduce large uncertainties into this estimate, as noted above.

(85) Lovett, E. G.; D'Avignon, D. A.; Holtzer, M. E.; Braswll, E. H.; Zhu, D.; Holtzer, A. *Proc. Natl. Acad. Sci. U.S.A.* **1996**, *93*, 1781−1785. Holtzer, M. E.; Holtzer, A. *Biopolymers* **1992**, *32*, 1589−1591.

(86) Manning, M. C.; Illangasekare, M.; Woody, R. W. *Biophys. Chem.* **1988**, *31*, 77−86.

(87) Chakrabartty, A.; Kortemme, T.; Padmanabhan, S.; Baldwin, R. L. *Biochemistry* **1993**, *32*, 5560−5565.

value. The isodichroic wavelength thus must lie near the center of this range, and $[\theta]_{isodichroic}$ is close to the mean of the values for $[\theta]_U$. As described in the Experimental Section, for any plausible temperature-dependent values of these limiting parameters, the isodichroic point in fact lies within the exceptionally narrow wavelength range of 202.0 to 203.0 nm, with likely values for $[\theta]_{isodichroic}$ lying between -12 and -24×10^3 deg cm^2 dmol^{-1}. The full extent of this latter range is sampled if one assumes the largest plausible values for $[\theta]_{H,192}$ and $[\theta]_{H,208}$. The least intense values of $[\theta]_{isodichroic}$ result from the values of $[\theta]_U$ that are observed at high temperatures.

This modeling predicts that if a large range of temperatures is used to construct a CD manifold and $[\theta]_U$ is characterized by a normal temperature dependence, the isodichroic point will unravel slightly at higher temperatures. Park et al. have noted this effect and cited the temperature dependence of $[\theta]_U$ as its cause.[88] Relying on a CD database measured for helical designer peptides and tropomyosins, Holtzer and Holtzer have calculated experimental values for $[\theta]_{isodichroic}$. Rabbit tropomyosins gave a value of -13.5 (SD 0.1) $\times 10^3$ deg cm^2 dmol^{-1}, and values ranging from -12 to -20×10^3 deg cm^2 dmol^{-1}were found for a series of homopolymers and designer peptides.[11] These are clearly consistent with our modeling ranges.

We conclude that the values for $\lambda_{isodichroic}$ and for $[\theta]_{isodichroic}$ are largely determined by the gross features of limiting CD spectra for helices and unstructured peptides and are relatively insensitive to small conformational effects. They probably can be used to detect peptides or proteins for which limiting helical and unordered CD spectra are markedly abnormal, but for commonly encountered peptides, neither parameter can be used to diagnose unusual temperature dependences of CD spectra for limiting helical or unordered conformers. The presence of the isodichroic point of course remains a necessary condition for two-state analysis of helical peptides, but it is relatively insensitive as a sufficient condition.

If an isodichroic point appears in a helical manifold near 203 nm, can one conclude that a sheet conformation makes an insignificant contribution to the conformational population? Sheet ellipticities vary significantly,[86] and isolated examples show $[\theta]_{203}$ values close to limits for unordered and helical spectra.[17] Clearly, an isodichroic point cannot exclude these anomalies. We based our modeling on the classical sheet spectrum for solubilized, aggregated polylysine.[1b] Using a locally linear model similar to that employed in the above calculation, we conclude that within the limits of CD measurement errors, an isodichroic point can appear near 203 nm in the presence of as much as 20% of sheet conformations. More sensitive physical methods such as light scattering, FTIR, or resonance Raman spectroscopy are probably more appropriate analytical tools for setting limits on the abundance of sheet conformations.

Helical manifolds can exhibit isodichroic points that deviate in wavelength or intensity from the Holtzer standard. CD manifolds for very weakly helical peptides not infrequently show isodichroic points with exceptionally weak ellipticities in the region of 203−210 nm.[89] Conceivably in these cases, the spectra in this region are dominated by unstructured conformations with unusual $[\theta]_U$ values. Although the spectra that define a classic isodichroic point exhibit a wide range of slope values at that point, as seen in the model manifold of Figure 1, manifolds with small slope variations are frequently encountered. In extreme cases, a manifold exhibits an isodichroic region in the range 198−203 nm that is similar in appearance to an extended horse tail, as in Figure 11E.[90] Analysis shows that in this case a 55 °C temperature change produces only a small change in $[\theta]_{208}$ and thus in FH. Horsetails at 203 nm may thus be diagnostic of peptide helicity that is relatively insensitive to the progress variable.[91] Horsetails with temperature-invariant $[\theta]$ over the 195−203 nm region also characterize manifolds for highly helical peptides that exhibit a temperature or additive-dependent oligomerization to form helix bundles, with characteristic changes in the 205−230 nm region.[92] A more serious interpretational problem results with temperature-dependent CD manifolds of peptides that contain separate helical and nonhelical regions which contribute independently to the experimental $[\theta]$. Although $[\theta]_H$ is large and positive at short wavelengths, its contribution decreases as the helix melts, but at higher temperatures the intensity of the negative $[\theta]_U$ decreases. Depending on the relative lengths of the two regions, as helix melting occurs these opposing effects can result in either an increase or a decrease in the negative intensity of $[\theta]_{exp}$ for wavelengths below 203 nm.

Quantitative estimation of the magnitudes of these effects is currently hampered by the dearth of model spectra for unordered peptides of substantially varying amino acid composition and sequence. The reported models for CD spectra of unordered peptide conformations are primarily derived from short lengths of homopeptide sequences, from helix-destabilized homopeptide sequences, and from medium-length helices interrupted by central proline residues.[93] These may not be representative of the spectra of unordered conformations of more typical heteropeptide sequences and for those rich in helix-weakening amino acids such as Ser, Thr, Asn, Asp, and His that are noted for their capacity to form hydrogen bonded structures with the neighboring peptide backbone, with addition of corresponding local CD signatures to $[\theta]_U$.

Helical propensities are often assigned by comparisons of the CD spectrum for a highly helical host peptide with that of a host−guest site mutant. Because a two-state helix-coil model underlies quantitative calculation of FH values and helical propensities from CD spectra, rigorously the resulting pair of CD spectra must be related by a simple similarity transformation, as in Figure 1. The manifold formed by combining the host spectrum with a series of spectra for its site mutants must show a normal isodichroic point if the guest has no other effect than a change in FH.

For guests that perturb ellipticity slightly, this behavior is frequently observed.[94] For larger perturbations, isodichroic

(88) Park, S.-H.; Shalongo, W.; Stellwagen, E. *Protein Sci*. **1997**, *6*, 1694−1700.
(89) Reily. M. D.; Thanabal, V.; Omecinsky, D. O. *J. Am. Chem. Soc*. **1992**, *114*, 6251−6252. Klee, W. A. *Biochemistry* **1968**, *7*, 2731−2736.
(90) The horsetail appearance is deceptive. In a region of high slope, the eye easily confuses distance between adjacent CD curves along a line normal to them with the proper, much larger magnitude of change of the ordinate $[\theta]$.
(91) Wen, D. I.; Laursen, R. A. *J. Biol. Chem.* **1992**, *267*, 14 102−14 108. Fiori, W. R.; Lundberg, K. M.; Millhauser, G. L. *Nature Struct. Biol*. **1994**, *1*, 374−377.
(92) Ho, S. P.; DeGrado, W. F. *J. Am. Chem. Soc.* **1987**, *109*, 6751−6758. Zhou, N. E.; Zhu, B.-Y.; Kay, C. M.; Hodges, R. S. *Biopolymers* **1992**, *32*, 419−426.
(93) Merutka, G.; Lipton, W.; Shalongo, W.; Park, S.-H.; Stellwagen, R. *Biochemistry* **1990**, *29*, 7511−7515.

points are frequently absent.[55b,95] Two of these cases are particularly striking. In 1990, Lyu et al.[47a] carried out a CD study of a host−guest manifold in which 10 guests were sited as replacements for the central trialanine sequence in the capped peptide succinyl$YSE_4K_4A_3E_4K_4NH_2$. The host and the Lys, Met, and Gln mutants gave highly helical CD spectra with an isodichroic point near 201 nm; the Thr, Asn, and Gly mutants gave less intense helical CD spectra and shared a more intense isodichroic point at 203 nm. A middle group of mutants derived from Ile, Val, and Ser failed to show an isodichroic point. The authors suggested differing effects of these guests on $[\theta]_U$ as a plausible explanation. A 1996 study by Liu et al.[95] examined the effects of three identical guest substitutions by V, F, S, T, and G at sites 6, 12, and 20 in the host peptide HK_2A_{12}-$WA_6K_4NH_2$. Large differences in the intensity of CD ellipticity were seen in water, in which no isodichroic point was detected, but in water containing 10 mM SDS, all peptides exhibited highly helical CD spectra, and an isodichroic region was observed. Although possible aggregation may have complicated interpretation of the CD spectra in water alone, it is noteworthy that in both these examples the CD manifold appears to be well-behaved provided the ellipticity of the host peptide is changed only slightly by the guest substitutions. It would appear that small CD changes that result from host−guest substitutions can probably be reliably interpreted to yield helical propensities, but quantitative helicity analyses of highly perturbed CD spectra may contain significant hidden errors.

What remains to be done to improve the accuracy of interpretation of the CD spectra of peptides in solution? Resolution of the issues outlined in the concluding section of the body of this report is a first step. In addition, tests to establish the role of changes in ellipticities of the unstructured states are long overdue. Finally, it is essential to back up any quantitative conclusions derived from CD spectra of peptides with independent analyses of data derived from other helicity tools. For convenience and ease of measurement, CD is unrivaled as a research tool, but much effort remains to realize its full promise as a precision measure of helicity, particularly for the important but difficult case of free helical peptides in solution.

Experimental Section

Solutions were prepared using 18.2 MΩ water obtained from a Millipore Gradient A10 purification system. Ethylene glycol EG (Aldrich spectroscopic grade) and trifluoroethanol (Aldrich > 99.5%) were used without purification. Perchlorate solutions were prepared as 0.1 M in $NaClO_4$ and adjusted to pH 1.0 (pH meter) by addition of $HClO_4$ yielding total $[ClO_4^-]$ of 0.2 M.

Polyalanine peptides,[9] $(Ala_4Lys)Ala_2NH_2$ peptides,[4] and the capped peptide[55c,57] $Ac^{\beta}DHelA_8\beta InpK_2WNH_2$ were prepared, purified, and characterized as previously reported.[55c] CD spectra were measured on an Aviv 62DS spectrometer equipped with a thermoelectric temperature controller and calibrated by literature procedures.[96] For the spaced, solubilized polyalanines $WK_4Inp_2{}^tLA_n{}^tLInp_2K_4NH_2$, five successive CD spectra were measured at 1.0 nm bandwidth and 0.5 nm step size in the wavelength interval 295−255 nm after temperature equilibration (12 min); their average was corrected for cell blank ellipticity, and the resulting spectra were smoothed using polynomial fitting software (Aviv 62DS version 4.0s). CD spectra at temperatures below −20 °C were measured by pumping ethanol chilled by a Haake DC50−K75 circulation bath through a 5 mm jacketed Hellma quartz cylindrical cell; the CD cell compartment was maintained under dry nitrogen atmosphere to prevent condensation, and temperatures within the cell were monitored by a Digi-Sense thermometer equipped with an 0.064 mm dia. probe containing a thermocouple. Spectra were corrected using a baseline taken at −50 °C, and 60% w/w EG−water mixtures were prepared by dilution of the aqueous stock with 76% w/w EG−water.

As reported,[9] the concentrations were assigned from the indole chromophore of Trp using a double-beam Varian Cary 100 Bio UV−vis spectrometer. CD and UV spectra were measured in 10 mm Hellma QS strain-free suprasil cells. Electrospray MS of CD solutions were measured using a Waters Micromass AMD 4000, yielding *m*/*z* ratios within 0.75 mass units of the expected values.[9] The peptides $AcHel(A_4K)_4A_2NH_2$ and $(A_4K)_4A_2NH_2$ were characterized by amino acid analysis and MALDI-MS. Concentrations of aqueous solutions for these peptides were determined by amino acid analysis and quantitative ninhydrin analysis using external and internal standards, as reported previously.[4] Values of $[\theta]$ used in calculating parameters of Figure 5 were obtained by averaging experimental CD data over 1.0 nm ranges, centered at 208 and 222 nm. For parametric correlations based on literature data, published CD manifolds were enlarged by xerography, a linear horizontal and vertical grid was superimposed, and values of $[\theta]_{222}$ and $[\theta]_{208}$ were estimated to three significant figures.

Lifson−Roig Modeling for A_{28} of the Magnitude of Curvature in Slopes of Parametric $[\theta]_{222}$-$[\theta]_{208}$ Plots that results from the Temperature Dependence of $[\theta]_{U,222}$. The model was based on five assumptions. Of the four limiting ellipticities that define the slope *B* of eq 2, three are taken as temperature independent, but the residue ellipticity $[\theta]_{U,222}$ for the unstructured state was assigned the temperature dependence shown in Figure 5. The corresponding $[\theta]_{U,208} = -7$ (in units of 10^3 deg cm^2/dmol). The limiting helical ellipticities $[\theta]_{H,222}$ and $[\theta]_{H,208}$ are equal and length dependent; but for a partially helical conformation containing a helical region of length i they have the value $-44(1-2.5/i)$. To carry out the calculation, a correspondence must be set up between *w* values and temperatures at which $[\theta]_{U,222}$ was measured. The limiting $[\theta]_{U,222}$ at 5 °C and 60 °C were linked respectively to *w* values of 1.4 and 1.07, obtained by previous modeling of $[\theta]_{exp,222}$ data at these temperatures.[9] Intermediary corresponding values were set by linear interpolation. In accord with common usage, the parameters v and t were set equal to 0.048. As reported previously,[55c] an (8 × 8) matrix was used to calculate state sums ss for Ala_{28}, using 0.77 as the capping parameter[50] for the terminal ^{t}L residues. The resulting state sum polynomial is then used to calculate mole fractions of conformations that are nonhelical χ_{nonh} or that contain helical regions of length *i*. Equation 6 gave calculated values $[\theta]_{calcd,\lambda}$ for the pair $\lambda =$ 208 and 222; these contain ellipticity contributions from both helical and unstructured α-carbons

$$[\theta]_{\lambda,calcd} = [\theta]_{U,\lambda}\cdot\chi_U + \frac{1}{28}\cdot\sum_{i=3}^{28}(i\cdot[\theta]_{H_i,\lambda} + (28-i)\cdot[\theta]_{U,\lambda})\chi_{H,i} \quad (6)$$

Twelve pairs of values of $[\theta]_{calcd,222}$ and $[\theta]_{calcd,208}$ were obtained from eq 6 by calculating χ_{nonh} and $\chi_{h,i}$ using the Lifson−Roig algorithm and varying the helical propensity w from 1.07 to 1.40 at intervals of 0.03. The corresponding required values of $[\theta]_{U,222}$ are given by $-20.7 + 15.15$ w. A parametric plot of these pairs is shown in Figure 17. Although linear by casual visual inspection, analysis reveals slight convex upward curvature. In Tables 1−5, a relative error parameter expressed as the percentage $100\sigma_{linear}/\langle[\theta]_{222}\rangle$ was used as a quantitative measure of relative error in slope. The value obtained for the plot of Figure 17 is −0.75%, which is comparable to that of Figure 6 for the linear parametric plot of the dimeric helical tropomyosin of Mo et al.,[25] but three times smaller than the value observed for the curved parametric plot for A_{28} shown in Figure 3. In the body of the text, we defined

(94) Padmanabhan, S.; York, E. J.; Gera, L.; Stewart, J. M.; Baldwin, R. *Biochemistry* **1994**, *33*, 8604−8609. Padmanabhan, S.; Baldwin, R. L. *Protein. Sci.* **1994**, *3*, 1992−1997.
(95) Liu, L.-P.; Li, S.-C.; Goto, N. K.; Deber, C. M. *Biopolymers* **1996**, *39*, 465−470.
(96) Chen, G. C.; Yang, J. T. *Anal. Lett.* **1976**, *10*, 1195−1207.

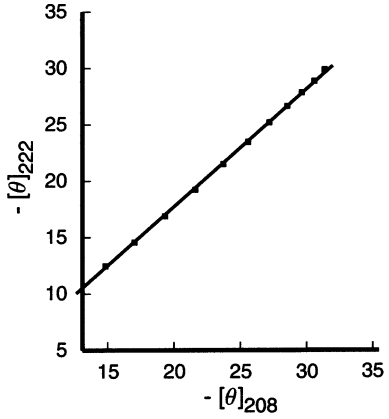

Figure 17. Calculated model data testing the effect of the contribution of the known temperature dependence of $[\theta]_{U,222}$ to the parametric slopes of an A_{28} peptide with temperature dependent *w* values as previously reported. Visual comparison of this Figure and the experimental data of Figure 3 shows that curvature resulting from the temperature dependence of $[\theta]_{U,222}$ is insufficient to account for the slope changes of Figure 3. Ordinate units: 10^3 deg cm^2 dmol^{-1}.

2.5% as the lower limit that defines presence of curvature. This bound is set by model calculations based on eq 5 in which plausible random measurement errors are added to the calculated values of $[\theta]_{222}$. The curvature parameter $\Delta B/(\Delta T \langle B \rangle)$ for Figure 17 is -3.1×10^3; again, three to four times smaller than that observed for our archetype curvature examples of A_{28} and $AcHel(A_4K)_4A_2NH_2$. We conclude that for simple helical peptides in aqueous solution, the magnitude of the temperature dependence of $[\theta]_{U,222}$ is insufficient to explain the curved parametric ellipticity plots that are characteristic of alanine-rich peptides.

Two partially compensating temperature effects contribute to the correlation of Figure 17; the major effect is the temperature dependence of $[\theta]_{U,222}$; the second effect is the temperature dependence of $[\theta]_H$ that is implicit in eq 6. Repeating the Lifson−Roig calculation using a constant value for $[\theta]_{U,222}$ and correlating ellipticities yields a curvature parameter of $+ 0.7 \times 10^3$ that is characteristic of the second effect. This will not contribute to parametric ellipticity correlations for highly structured helices characteristic of folded helical proteins or helical coiled-coils.

$WK_4Inp_2{}^tLA_4{}^tLK_{4-}NH_2$ as a Model for the Temperature-Dependent CD Manifold for Unstructured Alanines. Previously, we have reported CD data depicted in Figure 5 for the above peptide, whose residue content is eight K, four A, two ^{t}L, four Inp, and one W. The achiral Inp residues cannot contribute to the molar CD ellipticities. Previously, we have shown[9] that replacement of the $Inp_2{}^t$L and ^{t}LInp_2 spacing sequences by pairs of Inp_3 spacers has an insignificant effect on ellipticity; implying that the ^{t}L residues are not significant contributors to the molar ellipticity of this peptide. For the purposes of calculating residue ellipticities, we define the effective length of the peptide as twelve residues, comprising the four A and eight K residues. This definition is likely to set an upper bound on the intensities and temperature dependences of $[\theta]_U$ because extrapolation of the molar ellipticities of the series $WK_nInp_2{}^tLA_4{}^tLK_nNH_2$ where $n = 2$ through 7 to $n = 0$ suggests that the residue ellipticity for an unstructured Ala residue is less intense than that of a Lys. For this reason, all estimates of the effects of the temperature dependences of $[\theta]_{U,222}$ on parametric curvature are likely to be overestimated.

Acknowledgment. Fellowship support from the Swiss National Science Foundation (P.W.) financial support from NIH Grant No. 5 R01 GM 13453 (J.M.), and NSF Grant No. 9121702-CHE (W.S., R.J.K.) and from Pfizer Research are gratefully acknowledged.

JA0275360